ONLINE SUPPLEMENT

Table of content:

1. SUPPLEMENTARY METHODS (WITH REFERENCES)

Animal Models of Intrahepatic Cholangiocarcinoma. 10 μg *pT3-EF1α-myrAkt-HA*, 20 μg of *pT3-EF1α-Myc-N1ICD/pT3-EF1α-Flag-YAP1 S127A* and 60 μg mg of *pCMV-Cre (or pCMV-empty)*, or 10 μg *pT3-EF1α-myrAkt-HA* and 20 μg of *pT3-EF1α-Sox9*, or μg mg of *pT3-EF1α-myrAkt-HA-sh-Luciferase*, 20 μg of *pT3-EF1α-Myc-N1ICD, or* 10 μg of *pT3-EF1α-myrAkt-HA-Sh-Yap1*, 20 μg of *pT3-EF1α-Myc-N1ICD*, or 10 μg of *pT3-EF1α-myrAkt-HA-Sh-Dnmt1*, 20 μg of *pT3-EF1α-Myc-N1ICD, or* 10 μg of *pT3-EF1α-myrAkt-HA*, 20 μg of *pT3-EF1α-Myc-N1ICD,* 60 μg *of pT3-EF5α-Dn-TEAD, or* 20 μg of *pT3-EF1α-Myc-N1ICD, 60* μg *of pT3-EF5α-Dn-TEAD, or* 10 μg of *pT3-EF1α-myrAkt-HA-sh-Yap1*, 20 μg of *pT3-EF1α-Myc-N1ICD*, 10 μg and 40 μg of *pT3-EF1α-Dnmt1-V5, or* 10 μg of *pT3-EF1α-myrAkt-HA*, 20 μg of *pT3-EF1α-Myc-N1ICD, 60* μg *of pT3-EF5α-Dn-TEAD, 40* μg *of pT3-EF1α-Dnmt-V5,* or 10 μg of *pT3-EF1α-myrAkt-HA-sh-Luciferase*, 20 μg of *pT3-EF1α-Myc-N1ICD* and 40 μg of *pCMV-empty*, or 10 μg of *pT3-EF1α-myrAkt-HA-sh-Yap1*, 20 μg of *pT3-EF1α-Myc-N1ICD* and 40 μg of *pCMV-Cre*, or 10 μg of *pT3-EF1α-myrAkt-HA*, 20 μg of *Fbxw7ΔF*, or 10 μg of *Kras* G12D, 40 μg of *sh-p53* along with the transposase in a ratio of 25:1 were diluted in 2 ml of normal saline (0.9% NaCl), filtered through 0.22μm filter (Millipore), and hydrodynamically injected into the lateral tail vein of mice[1-3]. All animals were sacrificed between 2-5 weeks of plasmids injections unless otherwise indicated.

Immunohistochemistry (IHC). Mouse liver tissues were fixed for 48 h in 10% neutralized formalin (Fisher Chemicals), transferred into 70% ethanol and then dehydrated and

embedded in paraffin. For IHC, formalin-fixed sections were deparaffinized in graded xylene and ethanol and rinsed in PBS. For antigen retrieval, samples were microwaved for 12 min in pH 6.0 sodium citrate buffer (HA-tag, Myc-tag, panCK, SOX9) or pH 9.0 Tris-EDTA buffer (p-AKT) or DAKO (V5-tag), or were pressure cooked for 20 min in pH 9.0 Tris-EDTA buffer (YAP1 and HNF4α) or were autoclaved for 1 h in pH 9.0 Tris-EDTA buffer (DNMT1). After cooling, samples were placed in 3% H_2O_2 (Fisher Chemicals) for 10 min to quench endogenous peroxide activity. After washing with PBS, slides were blocked with Super Block (ScyTek Laboratories) for 10 min. Sections were incubated for overnight at 4C with the primary antibodies (Supplementary Table 2. Sections were then incubated with species-specific biotinylated secondary antibodies (EMD Millipore, Supplementary Table 2) for 1 h, at room temperature. Sections were incubated with Vectastain ABC Elite kit (Vector Laboratories) and signal was detected with DAB Peroxidase Substrate Kit (Vector Laboratories) followed by quenching in distilled water for 5 min. Slides were counterstained with hematoxylin (ThermoFisher Scientific), dehydrated to xylene (Fisher Chemicals) and coverslips applied with Cytoseal XYL (ThermoFisher Scientific).

Immunofluorescence. Paraffin embedded liver sections (5 μm thick) were deparaffinized using xylene (Fisher Chemicals) and rehydrated by incubating the slices in ethanol (100% and 95% v/v, each 3x5 min) and washed in PBS. Heat-induced epitope retrieval was performed for 20 min using a pressure cooker with pH 6.0 sodium citrate buffer. Sections were washed in PBS, permeabilized for 5 minutes with PBS/0.3% Triton X and blocked with PBS/0.3% Triton X/10% bovine serum albumin (BSA) for 45 minutes

at room temperature. Sections were incubated with primary antibodies in PBS/0.3% Triton X/10% BSA overnight at 4C. At the end of the incubation, sections were washed thrice and incubated with fluorochrome-conjugated secondary antibodies in PBS/0.3% Triton X/10% BSA for 1h at room temperature, then washed in PBS/0.1% Triton X 3 times. Liver sections were mounted using Prolong Gold Antifade w/DAPI (Invitrogen) and pictures were acquired using LSM700 confocal microscope and the Zen Software (Zeiss).

DNMT1 ChIP-seq analysis.

Chromatin Immunoprecipitation: Frozen liver tissue was sent to Active Motif Services (Carlsbad, CA) for ChIP-Seq. Active Motif prepared chromatin, performed ChIP reactions, generated libraries, sequenced the libraries, and performed basic data analysis. In brief, tissue was submersed in PBS + 1% formaldehyde, cut into small pieces, and incubated at room temperature for 15 minutes. Fixation was stopped by the addition of 0.125 M glycine (final). The tissue pieces were then treated with a TissueTearer and finally spun down and washed 2x in PBS. Chromatin was isolated by adding lysis buffer, followed by disruption with a Dounce homogenizer. Lysates were sonicated and the DNA sheared to an average length of 300-500 bp with Active Motif's EpiShear probe sonicator (cat# 53051). Genomic DNA (Input) was prepared by treating aliquots of chromatin with RNase, proteinase K and heat for de-crosslinking, followed by SPRI beads clean up (Beckman Coulter) and quantitation by Clariostar (BMG Labtech). Extrapolation to the original chromatin volume allowed determination of the total chromatin yield. An aliquot of chromatin (40 ug) was precleared with protein A agarose beads (Invitrogen). Genomic DNA regions of interest were isolated using antibodies against DNMT1 (Cell Signaling Technology, cat#:5032). Complexes were washed, eluted from the beads with SDS

buffer, and subjected to RNase and proteinase K treatment. Crosslinks were reversed by incubation overnight at 65C, and ChIP DNA was purified by phenol-chloroform extraction and ethanol precipitation.

ChIP-Sequencing (Illumina): Illumina sequencing libraries (a custom type, using the same paired read adapter oligonucleotides described by Bentley et al., (2008))[4] were prepared from the ChIP and Input DNAs on an automated system (Apollo 342, Wafergen Biosystems/Takara). After a final PCR amplification step, the resulting DNA libraries were quantified and sequenced on Illumina's NextSeq 500 (75 nt reads, single end). Reads were aligned to the mouse genome (mm10) using the BWA algorithm (default settings)[5]. Duplicate reads were removed and only uniquely mapped reads (mapping quality >= 25) were used for further analysis. Alignments were extended in silico at their 3'-ends to a length of 200 bp, which is the average genomic fragment length in the size-selected library, and assigned to 32-nt bins along the genome. The resulting histograms (genomic "signal maps") were stored in bigWig files. Peak locations were determined using the MACS algorithm (v2.1.0) with a cutoff of p-value = 1e-7[6]. Peaks that were on the ENCODE blacklist of known false ChIP-Seq peaks were removed. Signal maps and peak locations were used as input data to Active Motifs proprietary analysis program, which creates Excel tables containing detailed information on sample comparison, peak metrics, peak locations and gene annotations.

REFERENCES

1. Tao J, Zhang R, Singh S, et al. Targeting beta-catenin in hepatocellular cancers induced by coexpression of mutant beta-catenin and K-Ras in mice. Hepatology 2017;65:1581-1599.
2. Fan B, Malato Y, Calvisi DF, et al. Cholangiocarcinomas can originate from hepatocytes in mice. J Clin Invest 2012;122:2911-5.

3. Wang J, Dong M, Xu Z, et al. Notch2 controls hepatocyte-derived cholangiocarcinoma formation in mice. Oncogene 2018;37:3229-3242.
4. Bentley DR, Balasubramanian S, Swerdlow HP, et al. Accurate whole human genome sequencing using reversible terminator chemistry. Nature 2008;456:53-9.
5. Li H, Durbin R. Fast and accurate short read alignment with Burrows-Wheeler transform. Bioinformatics 2009;25:1754-60.
6. Zhang Y, Liu T, Meyer CA, et al. Model-based analysis of ChIP-Seq (MACS). Genome Biol 2008;9:R137.

2. SUPPLEMENTARY TABLES

Table S1: Summary of Patients with PSC and NASH used in the study.

Patient Record Number	Age	Sex	SOX9	pAKT S473	YAP	Hepatocyte DNMT1		Disease
						C	N	
PHR17-187	44	F	<20%	NEG	20-50%	100%	NEG	PSC
PHR17-315	39	M	NEG	NEG	<20%	100%	NEG	PSC
PHR17-318	32	M	20-50%	NEG	<20%	50%	20-50%	PSC
PHR17-340	47	F	20-50%	<20%	20-50%	100%	20-50%	PSC
PHR17-471	44	F	<20%	<20%	NEG	100%	<20%	PSC
PHS18-35	35	M	<20%	<20%	NEG	0%	NEG	PSC
PHR19-64	24	M	<20%	20-50%	20-50%	100%	<20%	PSC
PHR19-67	32	F	NEG	NEG	<20%			PSC
PHR19-74	50	M	<20%	20-50%	<20%	100%	<20%	PSC
PHR19-80	61	F	NEG	20-50%	<20%	100%	NEG	PSC
PHR16-107	67	M	<20%	<20%	<20%	0%	0	NASH
PHR17-50	73	F	<20%	NEG	<20%	0%	NEG	NASH
PHR17-114	53	F	20-50%	20-50%	NEG			NASH
PHR17-235	63	M	20-50%	20-50%	NEG	0%	NEG	NASH
PHR17-238	65	M	<20%	20-50%	NEG	50%	NEG	NASH
PHR17-247	61	M	<20%	NEG	<20%			NASH
PHR17-299	56	F	<20%	<20%	<20%	<20%	0	NASH
PHR18-25	68	F	20-50%	20-50%	<20%	50%	<20%	NASH
PHR18-219	62	F	<20%	NEG	<20%	<20%	<20%	NASH
PHR19-107	78	F	<20%	<20%	<20%	100%	NEG	NASH
NHL1029			NEG	NA	NEG			Healthy control liver
16-5566	54	F	NEG	NEG	NEG			Healthy control liver (underlying colon adenocarcinoma)
12-9718	60	M	NEG	NEG	NEG			Healthy control liver (underlying colon adenocarcinoma)

17-9693	49	F	NEG	NEG	NEG			Healthy control liver (underlying colon adenocarcinoma)
13-15397	54	F	NEG	NEG	20-50%			Healthy control liver (underlying colon adenocarcinoma)
14-2191	36	M	NEG	NEG	NEG			Healthy control liver (underlying colon adenocarcinoma)
PHS18-34295						0	NEG	Healthy control liver
PHS18-11592						0	NEG	Healthy control liver
PHS18-5904						0	NEG	Healthy control liver
PHS16-40535						0	NEG	Healthy control liver
PHS16-32066						0	NEG	Healthy control liver

Abbreviations: C-cytoplasmic; **N-** nuclear; **PSC-** Primary sclerosing cholangitis; **NASH-** Non alcoholic steatohepatitis

Table S2: Antibody List used in the study

Primary Antibodies:

Target	Species	Dilution	Source	Catalog Number
HA-tag	Mouse	1:50 (IHC)	Cell Signaling	CS2367
MYC-tag	Rabbit	1:100 (IHC)	Maine Medical Center Research Institute (mmcri)	Vli01
Pan-CYTOKERATIN (panCK)	Rabbit	1:200 (IHC)	Dako	Z0622
p-AKT	Rabbit	1:100 (IHC)	Cell Signaling	CS4060
SOX9	Rabbit	1:200 (IF) 1:2000 (IHC)	EMD Millipore	Ab5535
YAP1	Rabbit	1:100 (IF and IHC)	Cell Signaling	CS14074
HNF4α	Rabbit	1:100 (IHC)	Cell Signaling	CS3113
PCNA	Mouse	1:200 (IF)	Santa Cruz	sc-56
CK19	Rat	1:10 (IF)	DSHB	TROMA III
DNMT1	Rabbit	1:100 (IHC)	Abcam	ab188453

Secondary Antibodies:

Secondary Antibody	Species	Source	Catalog Number
Donkey anti-Rabbit IgG Biotin	Donkey	EMD Millipore	AP182B
Goat anti-Mouse IgG (H+L) Biotin	Goat	EMD Millipore	AP181B
Alexa-Fluor 555 Donkey anti-Rabbit IgG (H+L)	Donkey	Invitrogen	A31572
Alexa-Fluor 488 Donkey anti-Rat IgG (H+L)	Donkey	Invitrogen	A21208
Alexa-Fluor 647 Goat anti-Mouse IgG (H+L)	Goat	Invitrogen	A21236

Table S3: List of 200 genes used to estimate the genetic identity of *Akt-NICD*-ICC transcriptome with large clinical ICC cohort by Nearest Template Prediction assay

Number	Gene
1	TAGLN2
2	COL4A1
3	SPP1
4	CCND1
5	COL4A2
6	NRARP
7	ENC1
8	OSMR
9	KRT8
10	MKI67
11	ANXA2
12	ADCY5
13	PXDN
14	PODXL
15	TRIM47
16	DDR1
17	SOX9
18	SPON1
19	LBH
20	FSTL1
21	ANXA5
22	TPM4
23	SOX4
24	FLNA
25	B4GALT6
26	ELN
27	S100A11
28	ARL4C
29	CELSR2
30	KRT18
31	CD9

32	VCAM1
33	SLCO3A1
34	ADAMTS1
35	LAMA5
36	TUBA1A
37	CSRP1
38	TOP2A
39	FAR1
40	FADS3
41	EIF2AK3
42	TRIB2
43	SYNPO
44	DCDC2
45	TTYH1
46	CD63
47	DKK3
48	FAM118A
49	SH3PXD2B
50	JAG1
51	CLASP1
52	PTPN13
53	VIM
54	TGM2
55	EHF
56	PTK7
57	SCARA3
58	BCAM
59	BICC1
60	CKB
61	LMNA
62	PRC1
63	MARCKS
64	MCAM
65	BMP6
66	ENAH
67	STMN1
68	PFKFB4
69	RHBDF1
70	MAP1B

71	ADGRG1
72	SRC
73	MAP2
74	ANLN
75	VILL
76	HEYL
77	WLS
78	SMTNL2
79	GAS6
80	ELF3
81	ACTN1
82	PHLDA3
83	CENPF
84	PPP1R9B
85	MGAT5
86	GPC6
87	SERPINB6
88	ARHGEF10
89	VSIG10
90	COL1A1
91	GLS
92	ZNF703
93	AGPAT1
94	RACGAP1
95	CDKN1A
96	CDH15
97	SCD
98	LIG1
99	LTBP1
100	INHBB
101	CELA1
102	CYP4F12
103	FAM210A
104	CYP2D6
105	CDC14B
106	GNA12
107	RNF103
108	FECH
109	SUCNR1

110	AK3
111	IPMK
112	SULT1B1
113	PDK2
114	RETSAT
115	FBXO8
116	STAT5B
117	CAT
118	ERBB3
119	SLC25A42
120	SFXN5
121	PGM2
122	C16orf70
123	MN1
124	TYMP
125	GNS
126	CHUK
127	DHRS3
128	CMBL
129	TSC1
130	SELENBP1
131	RNF152
132	MOCS1
133	ABCD3
134	NFIX
135	SLC2A2
136	NDST1
137	RMND5A
138	CHPT1
139	FOXN3
140	ETFDH
141	HLF
142	GGACT
143	DYRK2
144	AL049629.2
145	ABCG8
146	IDH3B
147	HSD17B11
148	PXMP4

149	AGTR1
150	HSD11B1
151	INSIG2
152	KHNYN
153	ZCCHC24
154	CA1
155	PNPLA8
156	SNX29
157	CYB5R3
158	ALDH5A1
159	SDR42E1
160	NQO2
161	ACBD5
162	KHK
163	OPA1
164	DONSON
165	NAA60
166	TSPAN12
167	NPC1
168	FTCD
169	SEPHS2
170	UQCRB
171	ZFAND6
172	SCAP
173	PTTG1IP
174	MCC
175	PCTP
176	CYP4F8
177	RUFY3
178	ECM1
179	PRKD3
180	PPARGC1B
181	SASH1
182	DENND4A
183	FAM13A
184	HMGCS2
185	HYKK
186	SDHC
187	CA14

188	ACOT12
189	RILP
190	UGT1A1
191	CLDN1
192	NR1H4
193	ISOC1
194	NDUFA10
195	ACSL1
196	PAQR7
197	RNF125
198	PBLD
199	SLC6A9
200	MLXIPL

Table S4: List of 169 overlapped genes by integration of DNMT1 ChIP-seq and down-regulated in transcriptome profile

Number	Gene
1	GM4980
2	DENND4A
3	ACAD11
4	INCA1
5	ARRDC3
6	PTTG1IP
7	SMIM13
8	ACO1
9	AK2
10	APBA2
11	ATP5A1
12	ZFP36L1
13	C2
14	CHUK
15	PLK3
16	COX5A
17	CREM
18	CYP26A1
19	DCT
20	DYRK1B
21	EFNA3
22	EVI5
23	F8
24	FTL1
25	GAS1
26	GATA4
27	GCGR
28	GCH1
29	GOT2
30	AES
31	H2-KE6
32	FOXQ1
33	HHEX
34	HLX

35	IGFBP4
36	INSR
37	IRS1
38	MAFB
39	LHX2
40	ELOVL6
41	SLC8B1
42	AMACR
43	CRELD1
44	NPAS2
45	NPC1
46	NUMB
47	P2RY2
48	PDE9A
49	PITX3
50	RORA
51	SEMA6C
52	SOD1
53	CAMKK2
54	SLC25A38
55	SNED1
56	SDC4
57	SPRN
58	SH3BGRL2
59	ALDH4A1
60	SLC6A6
61	CECR5
62	TCP11L2
63	UGP2
64	GLTPD2
65	L2HGDH
66	VWA8
67	DLGAP1
68	LIMS2
69	ZADH2
70	ATRNL1
71	RNF103
72	C130074G19RIK
73	ZFP36

74	SLC25A25
75	PDK1
76	NUDT6
77	CREBL2
78	TUFM
79	ZBTB44
80	SH3BP5
81	GABBR2
82	GPRIN3
83	BAHCC1
84	GPHN
85	GPR157
86	BC024139
87	SLC25A10
88	MRPL39
89	ABCA8B
90	ABCC6
91	MARVELD1
92	ULK2
93	VPS13C
94	SLC35E2
95	DENND5B
96	ATP11C
97	MIA3
98	NR1D2
99	TLCD2
100	RBM33
101	DRC1
102	PDP2
103	CREG1
104	MN1
105	SHF
106	LRP3
107	SLC25A13
108	TNK2
109	ACAA2
110	GNPNAT1
111	EPB4.1L4B
112	ABCB10

113	NGLY1
114	GM6484
115	TSC1
116	ASB2
117	EEFSEC
118	ABHD6
119	1110001J03RIK
120	AAED1
121	NDUFB9
122	PYURF
123	FIGNL2
124	HINT3
125	ACADSB
126	LONP2
127	PXDC1
128	NDUFA6
129	PNPLA8
130	MMD
131	EEPD1
132	RNF125
133	DGAT2
134	ATG101
135	GCSH
136	0610030E20RIK
137	PCYT2
138	ELOVL5
139	DDAH1
140	HIST1H4H
141	CHN2
142	MPC2
143	MIPEP
144	CABYR
145	ARHGAP42
146	AMDHD1
147	PITPNC1
148	OSGIN1
149	LRPPRC
150	MBLAC2
151	PMPCB

152	SLC25A16
153	RHOX13
154	NMNAT3
155	GBE1
156	TBC1D30
157	TBC1D30
158	ARL5A
159	1700001C19RIK
160	FGGY
161	KLHL24
162	DOCK8
163	GRHPR
164	MND1
165	OCEL1
166	9430038I01RIK
167	CML2
168	PHLPP1
169	RDH10

Table S5: 320 upstream regulators for identified 169 overlapped genes (Table S4) predicted by IPA-URA tool

Upstream Regulator	Molecule Type	p-value of overlap
methylprednisolone	chemical drug	4.36E-07
INSR	kinase	7.17E-06
moxonidine	chemical drug	1.07E-04
CPT1B	enzyme	1.15E-04
mono-(2-ethylhexyl)phthalate	chemical toxicant	1.37E-04
D-glucose	chemical - endogenous mammalian	1.98E-04
IGF2BP2	translation regulator	2.75E-04
ANGPTL7	other	2.75E-04
methotrexate	chemical drug	3.22E-04
peoniflorin	chemical drug	3.27E-04
APP	other	3.71E-04
TP53	transcription regulator	4.07E-04
SMYD1	transcription regulator	4.71E-04
tert-butyl-hydroquinone	chemical reagent	4.91E-04
LONP1	peptidase	5.15E-04
PTPN1	phosphatase	5.43E-04
isobutylmethylxanthine	chemical toxicant	7.65E-04
NKX2-2-AS1	other	8.09E-04
USP28	peptidase	9.51E-04
LDHB	enzyme	9.51E-04
ABCB7	transporter	9.51E-04
INS	other	9.93E-04
metribolone	chemical reagent	1.03E-03
IGF2	growth factor	1.12E-03
CEBPA	transcription regulator	1.19E-03
DIO3	enzyme	1.23E-03
Ck2	complex	1.62E-03
IGF2R	transmembrane receptor	2.01E-03
CLOCK	transcription regulator	2.06E-03

GRB10	other	2.45E-03
sphingomyelin	chemical - endogenous mammalian	2.45E-03
GCG	other	2.53E-03
PNPLA2	enzyme	2.64E-03
beraprost	chemical drug	2.92E-03
NFU1	other	2.95E-03
NUPR1	transcription regulator	2.98E-03
WNT3A	cytokine	3.00E-03
UQCC3	other	3.12E-03
GNAQ	enzyme	3.51E-03
beta-carotene	chemical - endogenous mammalian	3.59E-03
streptozocin	chemical drug	3.78E-03
elaidic acid	chemical - endogenous mammalian	3.81E-03
pirinixic acid	chemical toxicant	3.96E-03
Cd2+	chemical toxicant	3.99E-03
DSCAM	other	4.11E-03
FFAR4	G-protein coupled receptor	4.59E-03
CG	complex	5.37E-03
topiramate	chemical drug	5.69E-03
PRKAG3	kinase	5.70E-03
miR-124-3p (and other miRNAs w/seed AAGGCAC)	mature microRNA	5.84E-03
TO-901317	chemical reagent	6.20E-03
leukotriene D4	chemical - endogenous mammalian	6.31E-03
HNF1A	transcription regulator	6.46E-03
raloxifene	chemical drug	6.60E-03
IGFBP2	other	6.64E-03
rosiglitazone	chemical drug	6.80E-03
RDH5	enzyme	6.83E-03
KLHL13	other	6.83E-03
KLHL9	other	6.83E-03
Gm13570/Gm4984	other	6.83E-03
JAKMIP1	other	6.83E-03

PISD	enzyme	6.83E-03
GRB14	other	6.83E-03
SNX5	transporter	6.83E-03
M6PR	transporter	6.83E-03
FAM13A	other	6.83E-03
diacetylbis(4-methylthiosemicarbazonato)copper(II)	chemical reagent	6.83E-03
MID-1	chemical reagent	6.83E-03
myrcene	chemical - endogenous non-mammalian	6.83E-03
cineole	chemical drug	6.83E-03
FOXA2	transcription regulator	6.83E-03
dexamethasone	chemical drug	6.93E-03
ZC3H12A	enzyme	7.09E-03
LEP	growth factor	7.33E-03
PHLPP1	enzyme	7.34E-03
DBP	transcription regulator	7.34E-03
GSK3A	kinase	7.34E-03
PRKCG	kinase	7.67E-03
RPA1	other	8.12E-03
POR	enzyme	8.14E-03
GnRH analog	biologic drug	8.17E-03
Esrra	transcription regulator	8.28E-03
HOXA9	transcription regulator	8.33E-03
IGF1	growth factor	8.48E-03
MAP4K4	kinase	8.78E-03
MECP2	transcription regulator	9.29E-03
PLN	transporter	9.59E-03
TRIM2	enzyme	9.78E-03
fenofibrate	chemical drug	1.04E-02
sirolimus	chemical drug	1.06E-02
TSPYL5	other	1.07E-02
MGP	other	1.07E-02
SULT1E1	enzyme	1.07E-02
diallyl trisulfide	chemical - endogenous non-mammalian	1.07E-02

BACH1	transcription regulator	1.09E-02
IL4	cytokine	1.09E-02
cyclic AMP	chemical - endogenous mammalian	1.09E-02
tributyltin	chemical reagent	1.13E-02
TINCR	other	1.16E-02
Z-LLL-CHO	chemical - protease inhibitor	1.18E-02
ESR2	ligand-dependent nuclear receptor	1.20E-02
mir-133	microRNA	1.22E-02
HNF4A	transcription regulator	1.24E-02
CD3	complex	1.25E-02
COMMD1	transporter	1.25E-02
IRS1	enzyme	1.29E-02
GNA14	enzyme	1.32E-02
CD 437	chemical drug	1.34E-02
ACLY	enzyme	1.35E-02
SRD5A1	enzyme	1.35E-02
SD 0006	chemical reagent	1.36E-02
LINC00667	other	1.36E-02
STARD4	transporter	1.36E-02
SOCS7	other	1.36E-02
USP46	peptidase	1.36E-02
PTPase	group	1.36E-02
TCDD-AHR	complex	1.36E-02
FBXW8	enzyme	1.36E-02
beta-apo-14'-carotenal	chemical - endogenous mammalian	1.36E-02
NKIRAS1	enzyme	1.36E-02
ME1	enzyme	1.36E-02
GABRG2	ion channel	1.36E-02
DNAJB1	transcription regulator	1.36E-02
bavachalcone	chemical reagent	1.36E-02
primaquine	chemical drug	1.36E-02
milrinone	chemical drug	1.36E-02
talarozole	chemical drug	1.36E-02

glipizide	chemical drug	1.36E-02
apo-13-lycopenone	chemical reagent	1.36E-02
apo-15-lycopenal	chemical reagent	1.36E-02
ZBTB7B	transcription regulator	1.37E-02
CD300LF	other	1.45E-02
NR4A1	ligand-dependent nuclear receptor	1.57E-02
miR-223-3p (miRNAs w/seed GUCAGUU)	mature microRNA	1.67E-02
CCL5	cytokine	1.69E-02
miR-7a-5p (and other miRNAs w/seed GGAAGAC)	mature microRNA	1.78E-02
N(G)-monomethyl-D-arginine	chemical - endogenous mammalian	1.78E-02
FOXO1	transcription regulator	1.79E-02
IFRD1	other	1.89E-02
PSEN1	peptidase	1.95E-02
beta-estradiol	chemical - endogenous mammalian	1.97E-02
ALDH1A2	enzyme	2.01E-02
NCOA4	transcription regulator	2.01E-02
IRS	group	2.03E-02
TAF3	transcription regulator	2.03E-02
DNAJA2	enzyme	2.03E-02
STARD5	transporter	2.03E-02
dapagliflozin	chemical drug	2.03E-02
PHYH	enzyme	2.03E-02
aurora kinase inhibitor III	chemical - kinase inhibitor	2.03E-02
FTMT	enzyme	2.03E-02
AFDN	other	2.03E-02
NEU1	enzyme	2.03E-02
RDH16	enzyme	2.03E-02
BRF110	chemical reagent	2.03E-02
CDD450	chemical drug	2.03E-02
actinomycin	chemical - endogenous non-mammalian	2.03E-02
quinine	chemical drug	2.03E-02

glyphosate	chemical toxicant	2.03E-02
TLE3	other	2.11E-02
AHCY	enzyme	2.13E-02
SCAP	other	2.24E-02
cinnamaldehyde	chemical toxicant	2.24E-02
bardoxolone	chemical drug	2.25E-02
Insulin	group	2.27E-02
PTGER4	G-protein coupled receptor	2.28E-02
RYR1	ion channel	2.38E-02
CA9	enzyme	2.38E-02
daunorubicin	chemical drug	2.38E-02
TRAP1	enzyme	2.45E-02
CD38	enzyme	2.47E-02
Stat3-Stat3	complex	2.51E-02
CEBPB	transcription regulator	2.51E-02
hydrocortisone	chemical - endogenous mammalian	2.52E-02
EGLN	group	2.52E-02
ST1926	chemical drug	2.52E-02
TSC2	other	2.57E-02
Hbb-b1	transporter	2.59E-02
GNB2	enzyme	2.64E-02
nicotinic acid	chemical - endogenous mammalian	2.64E-02
RARG	ligand-dependent nuclear receptor	2.66E-02
SKA3	other	2.70E-02
GPR55	G-protein coupled receptor	2.70E-02
tyrosine kinase	group	2.70E-02
MCU	ion channel	2.70E-02
CCDC3	other	2.70E-02
FDX2	transporter	2.70E-02
OPN3	G-protein coupled receptor	2.70E-02
MITF-p300/CBP	complex	2.70E-02
PX 478	chemical drug	2.70E-02
GH2	other	2.70E-02

FGD5-AS1	other	2.70E-02
mir-32	microRNA	2.70E-02
FDXR	enzyme	2.70E-02
HAP1	other	2.70E-02
AK4	kinase	2.70E-02
diamide	chemical reagent	2.70E-02
9-cis-retinal	chemical - endogenous mammalian	2.70E-02
thymeleatoxin	chemical toxicant	2.70E-02
MBTD1	other	2.77E-02
Immunoglobulin	complex	2.78E-02
DYSF	other	2.81E-02
methamphetamine	chemical drug	2.81E-02
lipopolysaccharide	chemical drug	2.88E-02
PRKN	enzyme	2.89E-02
HDL-cholesterol	complex	2.91E-02
CARM1	transcription regulator	2.91E-02
GNB1	enzyme	2.91E-02
BTG2	transcription regulator	2.91E-02
sucrose	chemical - endogenous mammalian	2.91E-02
HDAC3	transcription regulator	3.04E-02
ATP7B	transporter	3.05E-02
CTF1	cytokine	3.05E-02
GLI1	transcription regulator	3.14E-02
SAMMSON	other	3.19E-02
M344	chemical reagent	3.19E-02
dihydrotestosterone	chemical - endogenous mammalian	3.27E-02
N-nitro-L-arginine methyl ester	chemical drug	3.28E-02
propofol	chemical drug	3.34E-02
PAX5-ELN	fusion gene/product	3.34E-02
S-nitrosoglutathione	chemical toxicant	3.34E-02
PSEN2	peptidase	3.36E-02
inositol	chemical drug	3.37E-02
ginsenoside Re	chemical drug	3.37E-02

ZC3H10	other	3.37E-02
MPC1	transporter	3.37E-02
ALDH3A2	enzyme	3.37E-02
insulin detemir	biologic drug	3.37E-02
miR-202-3p (and other miRNAs w/seed GAGGUAU)	mature microRNA	3.37E-02
mir-191	microRNA	3.37E-02
BCAR3	other	3.37E-02
tofogliflozin	chemical drug	3.37E-02
Meis1	transcription regulator	3.37E-02
mini-GAGR	chemical reagent	3.37E-02
CB-PIC	chemical reagent	3.37E-02
chlorine	chemical toxicant	3.37E-02
SLC27A2	transporter	3.48E-02
pituitary adenylate cyclase-activating polypeptide	biologic drug	3.48E-02
NGF	growth factor	3.56E-02
trans-hydroxytamoxifen	chemical drug	3.57E-02
PPARGC1A	transcription regulator	3.59E-02
ethanol	chemical - endogenous mammalian	3.62E-02
HBA1/HBA2	transporter	3.63E-02
LRP5	transmembrane receptor	3.63E-02
ESRRB	transcription regulator	3.79E-02
thyroid hormone	chemical - endogenous mammalian	3.82E-02
uranyl nitrate	chemical toxicant	3.88E-02
HNRNPH1	other	3.94E-02
CUL4B	other	3.94E-02
NFIB	transcription regulator	3.94E-02
bafilomycin A1	chemical drug	3.94E-02
MTOR	kinase	3.96E-02
SERCA	group	4.03E-02
Cbp/p300-Maf-Nfe2l2	complex	4.03E-02
PGRMC2	transporter	4.03E-02
VANGL2	other	4.03E-02

GSK690693	chemical drug	4.03E-02
KCNIP2	transporter	4.03E-02
miR-137-3p (miRNAs w/seed UAUUGCU)	mature microRNA	4.03E-02
SRPK1	kinase	4.03E-02
NOCT	transcription regulator	4.03E-02
CAMK1	kinase	4.03E-02
BARD1	transcription regulator	4.03E-02
zonisamide	chemical drug	4.03E-02
GSK2837808A	chemical reagent	4.03E-02
Z-Leu-Leu-Leu-B(OH)2	chemical reagent	4.03E-02
methyllycaconitine	chemical toxicant	4.03E-02
N-retinylidene-N-retinylethanolamine	chemical - endogenous mammalian	4.03E-02
2,4,5,2',4',5'-hexachlorobiphenyl	chemical toxicant	4.06E-02
IRF4	transcription regulator	4.08E-02
topotecan	chemical drug	4.08E-02
doxorubicin	chemical drug	4.12E-02
palmitic acid	chemical - endogenous mammalian	4.17E-02
SCD	enzyme	4.22E-02
H2AX	transcription regulator	4.26E-02
ADRA1B	G-protein coupled receptor	4.26E-02
ADRA1D	G-protein coupled receptor	4.26E-02
n-3 fatty acids	chemical drug	4.26E-02
SREBF1	transcription regulator	4.28E-02
Rxr	group	4.33E-02
SPARC	other	4.33E-02
miR-1-3p (and other miRNAs w/seed GGAAUGU)	mature microRNA	4.35E-02
PAF1	other	4.42E-02
PDX1	transcription regulator	4.49E-02
ONECUT1	transcription regulator	4.50E-02
Hedgehog	group	4.58E-02
ZNF100	transcription regulator	4.68E-02
ZNF85	transcription regulator	4.68E-02

ZNF254	transcription regulator	4.68E-02
RASSF8	other	4.68E-02
ZNF431	transcription regulator	4.68E-02
USP29	peptidase	4.68E-02
ACIN1	enzyme	4.68E-02
PDE6B	enzyme	4.68E-02
COMT	enzyme	4.68E-02
RHEB	enzyme	4.68E-02
PDE3A	enzyme	4.68E-02
ZNF665	other	4.68E-02
ZNF528	other	4.68E-02
HOXC-AS3	other	4.68E-02
ZNF43	transcription regulator	4.68E-02
ZNF429	transcription regulator	4.68E-02
SORL1	transporter	4.68E-02
SENP2	peptidase	4.68E-02
GNMT	enzyme	4.68E-02
ZNF708	other	4.68E-02
thenoyltrifluoroacetone	chemical reagent	4.68E-02
HI-TOPK32	chemical reagent	4.68E-02
RORC	ligand-dependent nuclear receptor	4.71E-02
RICTOR	other	4.79E-02
IL5	cytokine	4.91E-02
inosine	chemical - endogenous mammalian	4.92E-02
MAP2K5	kinase	4.92E-02
ADRA1A	G-protein coupled receptor	4.92E-02
CTBP1	enzyme	4.92E-02
cisplatin	chemical drug	4.93E-02
KMT2D	transcription regulator	5.00E-02
quercetin	chemical drug	7.22E-02
acetaminophen	chemical drug	8.35E-02

3. Supplementary Figures and Legends

Figure S1

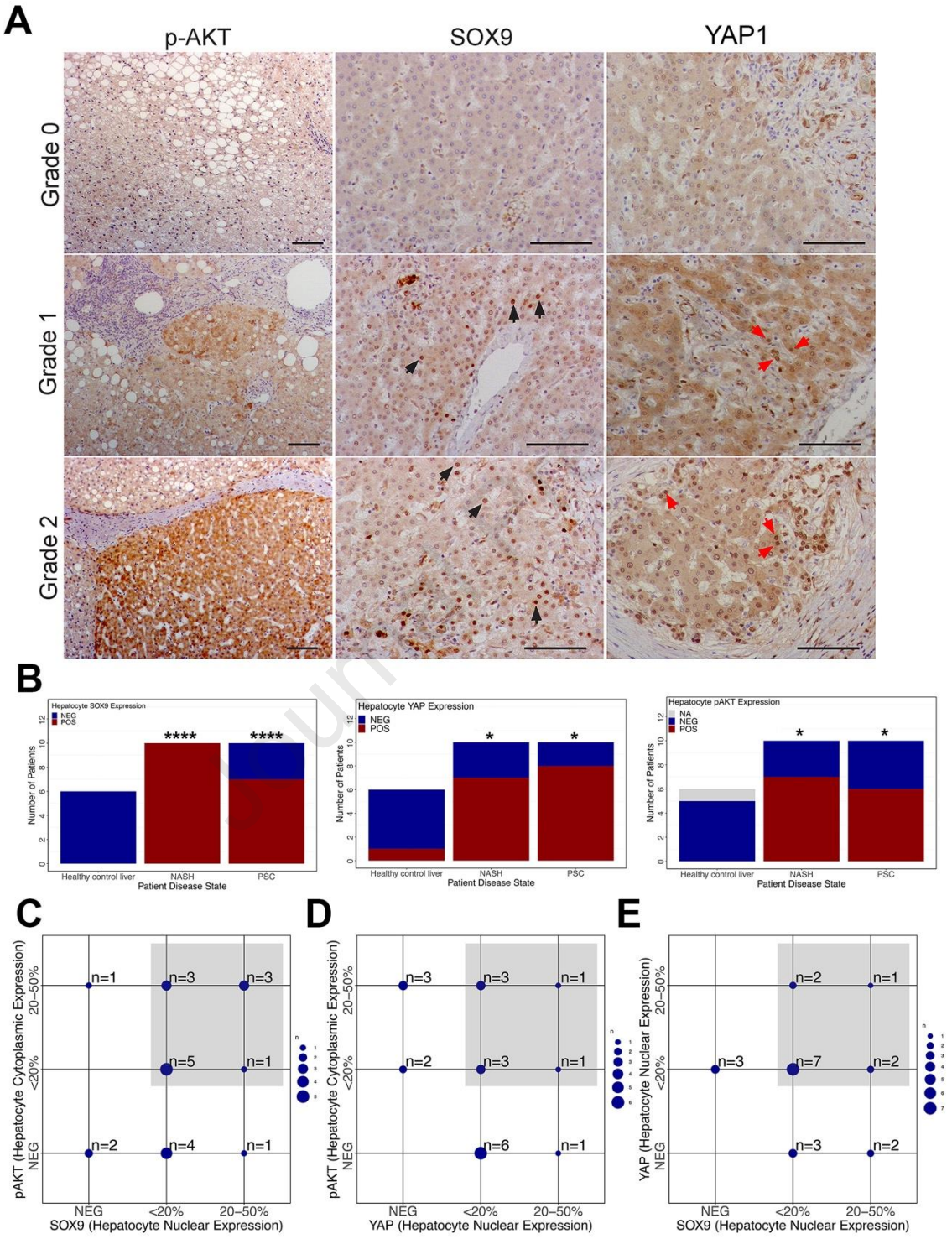

Figure S1. Activation of p-AKT, YAP1 and SOX9 in human liver diseases with higher risk for the development of ICC. (**A**) Representative human liver section images used for arbitrary scoring for p-AKT, SOX9 and YAP1 expression by IHC. Grade 0, no expression; grade 1< 20%; grade 2<50% (Grade 1 and 2 are considered positive). (**B)** Comparison of the number of patients with positive expression of SOX9, YAP1, or p-AKT in HCs shows an enrichment in positive HCs among PSC and NASH patients vs healthy controls. **(C-E)** Overlap in the expression of YAP1, SOX9, and p-AKT among patients with PSC and NASH shows most patients have at least 2 of 3 markers upregulated. Scale bars:100 µm. *p<0.05; ****p< 0.0001.

Figure S2

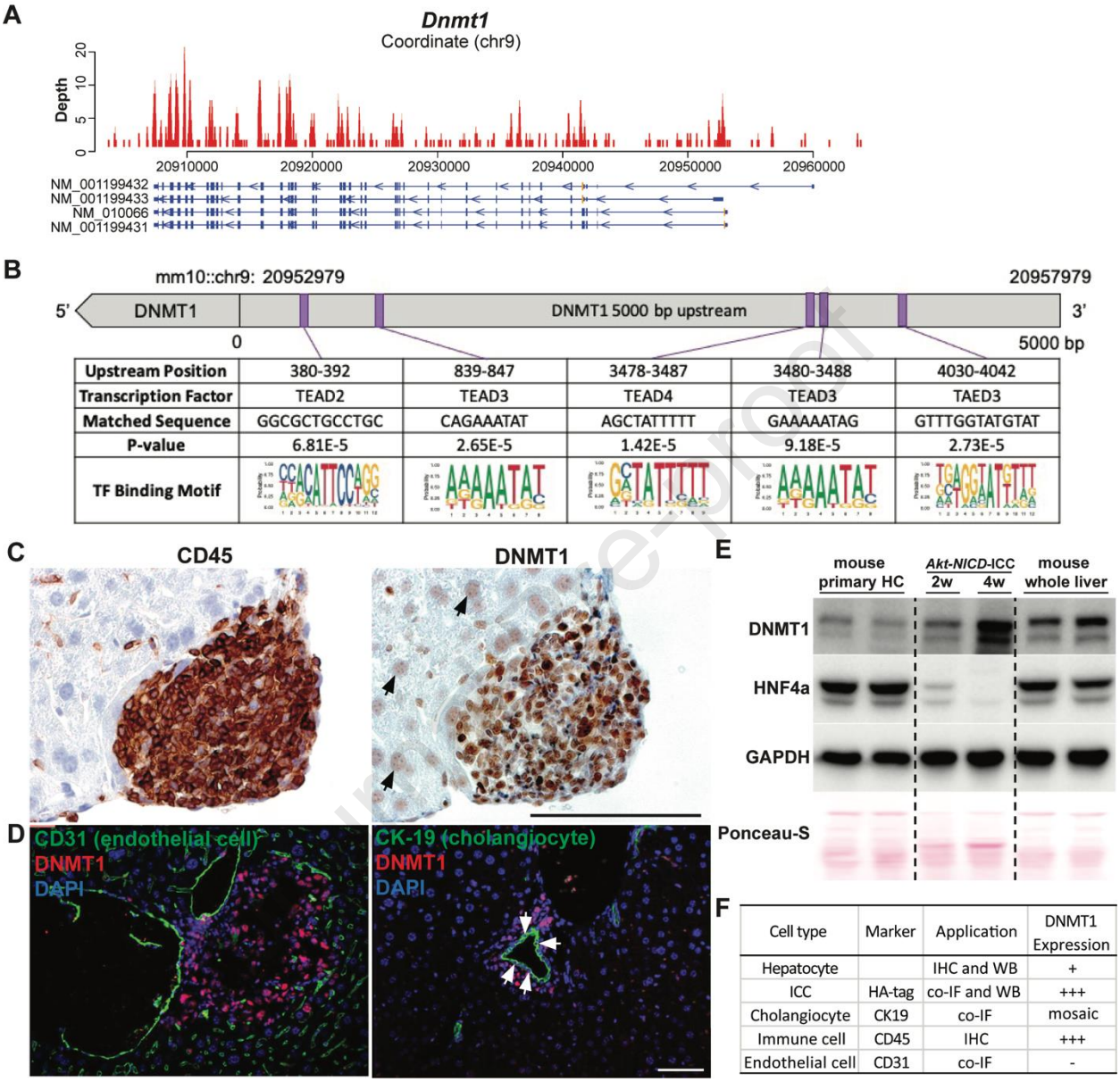

Figure S2. DNMT1 expression in mouse liver. (A) ChIP-seq data for TEAD4 binding sites on *Dnmt1* genomic regions are collected form GEO GSM2882182. **(B)** Predicted TEAD2/TEAD3/TEAD4 binding sites located at 5,000 bp upstream from *Dnmt1* transcription start site. **(C)** IHC staining for *Akt-NICD* KO ICC liver at 5 weeks post HDTVI showing strong DNMT1 expression in $CD45^{+}$ immune cells whereas weak expression in HCs (arrows). **(D)** Co-IF showing strong nuclear DNMT1 expression in

subset of CK-19+ cholangiocytes but not in CD31+ endothelial cells in the liver. **(E)** Representative WB from two independent experiment shows weak DNMT1 expression in HNF4a-enriched mouse primary HCs while strong augment of DNMT1 during transformation into ICC cells. **(F)** Table summarizing the DNMT1 expression pattern in diverse cell types in the liver. scale bar: 100 um.

Figure S3

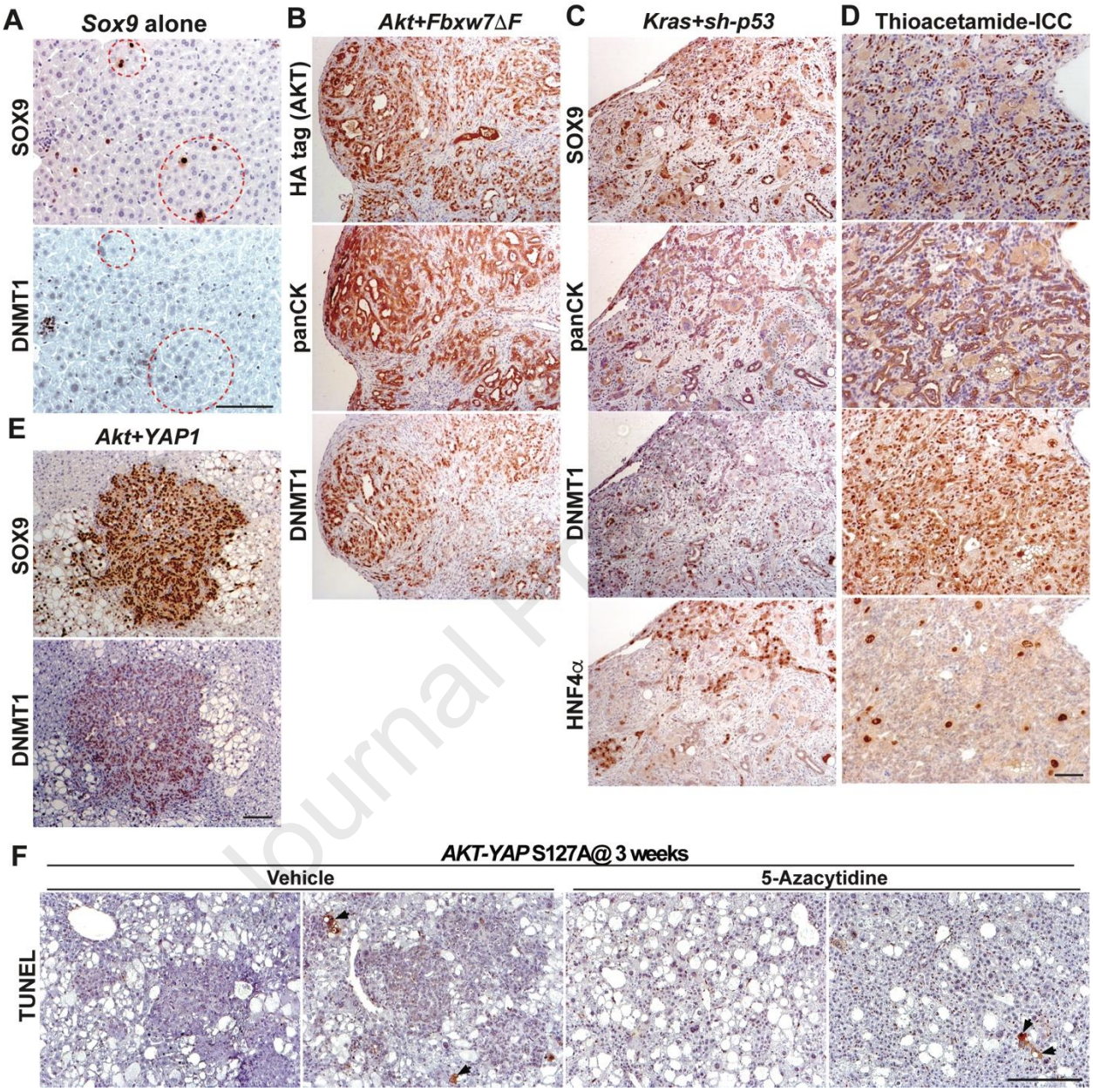

Figure S3. DNMT1 expression in HC-derived ICC models. (A) Representative IHC staining of *Sox9* expression plasmid-injected liver 3 weeks after injection showing absence of DNMT1 expression in *Sox9* singular-transduced HCs. **(B)** Representative IHC staining of liver from *Akt-Fbxw7ΔF*-driven ICC shows strong DNMT1 expression (100x). **(C)** Representative IHC staining of liver from *KRAS*-sh-*p53*-driven ICC shows strong

DNMT1 expression (100x). **(D)** Representative IHC staining of liver from *Akt-YAP*-driven ICC shows strong DNMT1 expression (100x). **(E)** Representative IHC staining of liver from TAA-administered mice at 24 weeks. IHC staining indicates panCK^{+};SOX9^{+};HNF4α^{-};DNMT1^{+} ICC with biliary morphology. **(F)** Representative TUNEL staining of liver from vehicle or 5-azacytidine-treated mice bearing *Akt-YAP1*-liver cancer at 3 weeks post HDTVI. Arrows indicate TUNEL^{+} cells. Scale bars:100 μm.

Figure S4

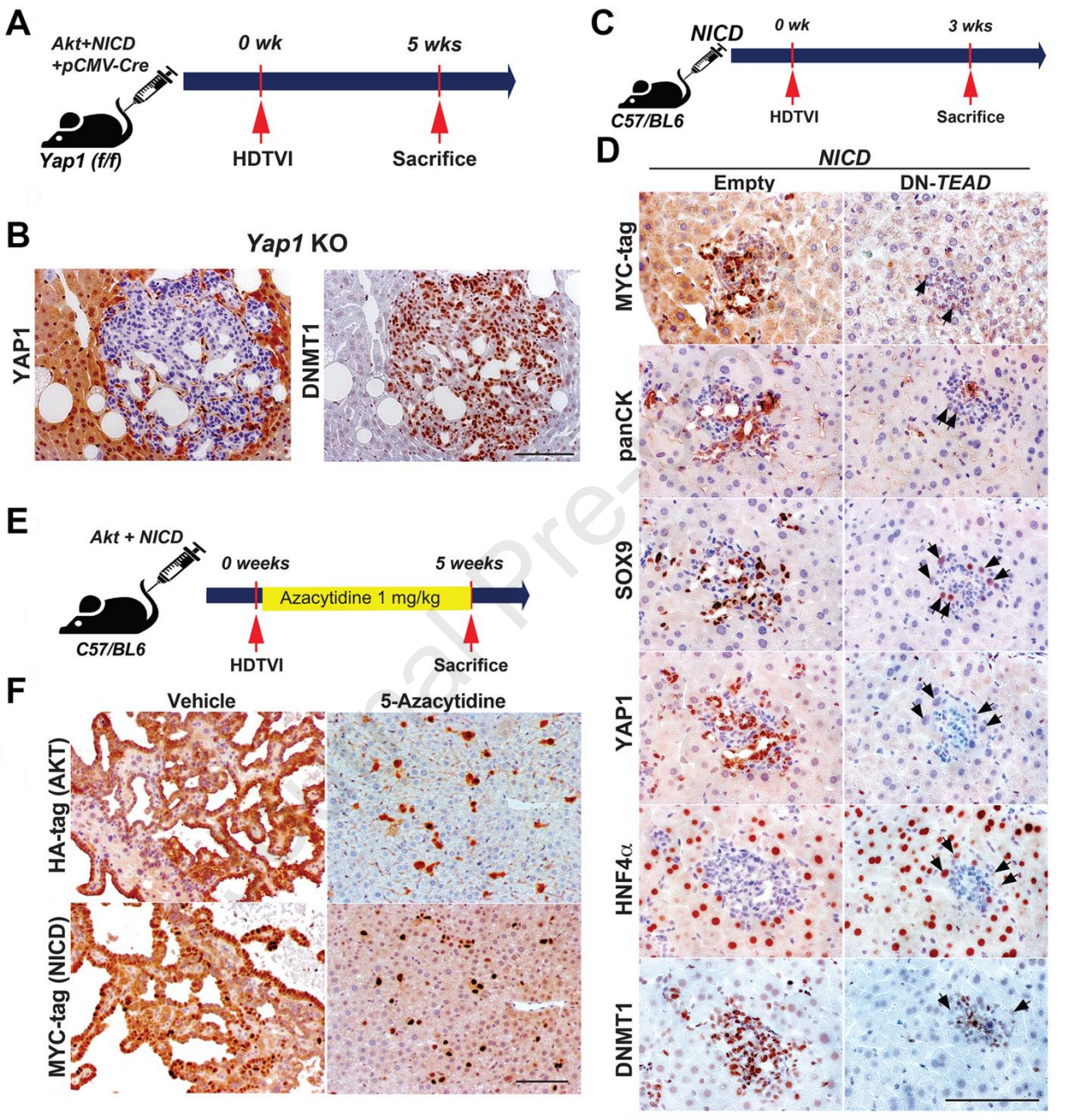

Figure S4. DNMT1 in HC-driven ICC. (A and B) Experimental design illustrating plasmids used for HDTVI, mice used in study and time-points analyzed. IHC staining for *Akt-NICD-Yap1* KO ICC at 5 weeks post HDTVI showing strong DNMT1 expression. **(C**

and D) Experimental design illustrating use of NICD alone or NICD + dn-TEAD plasmids for HDTVI and time-points analyzed. Representative IHC staining of *NICD-Empty* or *NICD*-DN-*TEAD* injected livers showing *NICD*-transfected cells (MYC-tag^{+}) with intact HC-to-ICC reprogramming with loss of HNF4α and gain of YAP, panCK and DNMT1. DN-*TEAD* livers showing *NICD*-transfected cells with defective HC-to-BEC reprogramming with continued HNF4α staining and absent of DNMT1 in YAP1^{-} HCs (black arrows). **(D)** Experimental design illustrating 5-Azacytidine treatment, plasmid used for HDTVI, mice used in study and time-point analyzed. **(E)** Representative IHC images for HA-tag (AKT), MYC-tag (NICD), and panCK showing dramatic tumor development in *Akt-NICD* WT livers and normal histology in 5-Azacytidine-treated livers at 5 weeks post HDTVI. Scale bars:100 µm.

Figure S5

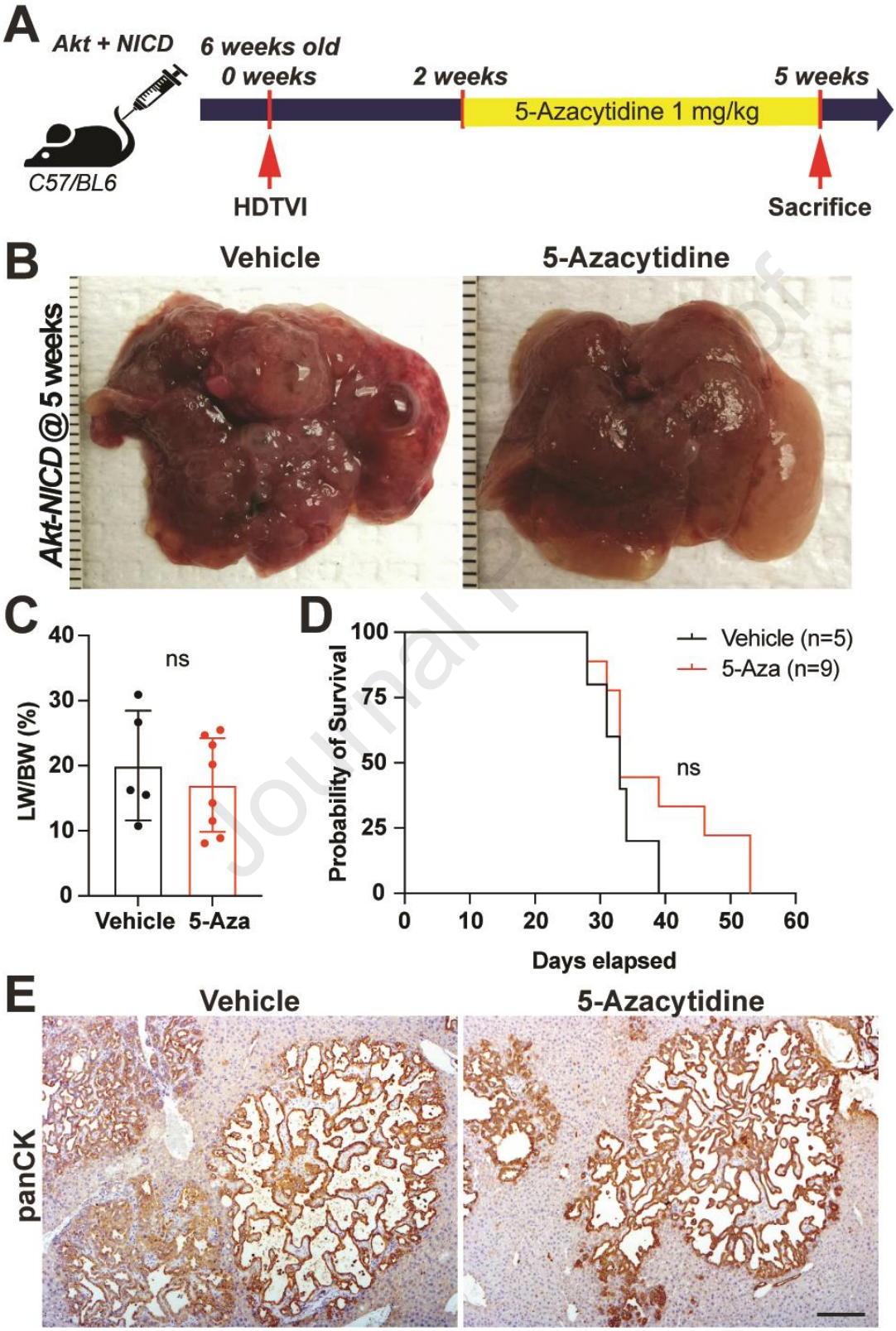

Figure S5: Pharmacologic DNMT1 inhibition does not reduce advanced AN-ICC tumor burden. (A) Experimental design illustrating 5-Azacytidine treatment, plasmids used for HDTVI, mice used in study and time-points analyzed. **(B)** Representative gross images show comparable *Akt-NICD* tumor development between Vehicle or 5-Azacytidine-treated livers at 5w post-injection **(C)** LW/BW ratio depicts comparable tumor burden in Vehicle or 5-Azacytidine-treated animals at 5w. **(D)** Kaplan-Meier survival curve showing comparable survival rate between Vehicle or 5-Azacytidine-treated mouse bearing AN-ICC**. (E)** Representative IHC images of 5w vehicle- or 5-Azacytidine-treated livers bearing *Akt-NICD*-driven ICC component positive for panCK. Ns, not significant; Scale bar: 100um.

Figure S6

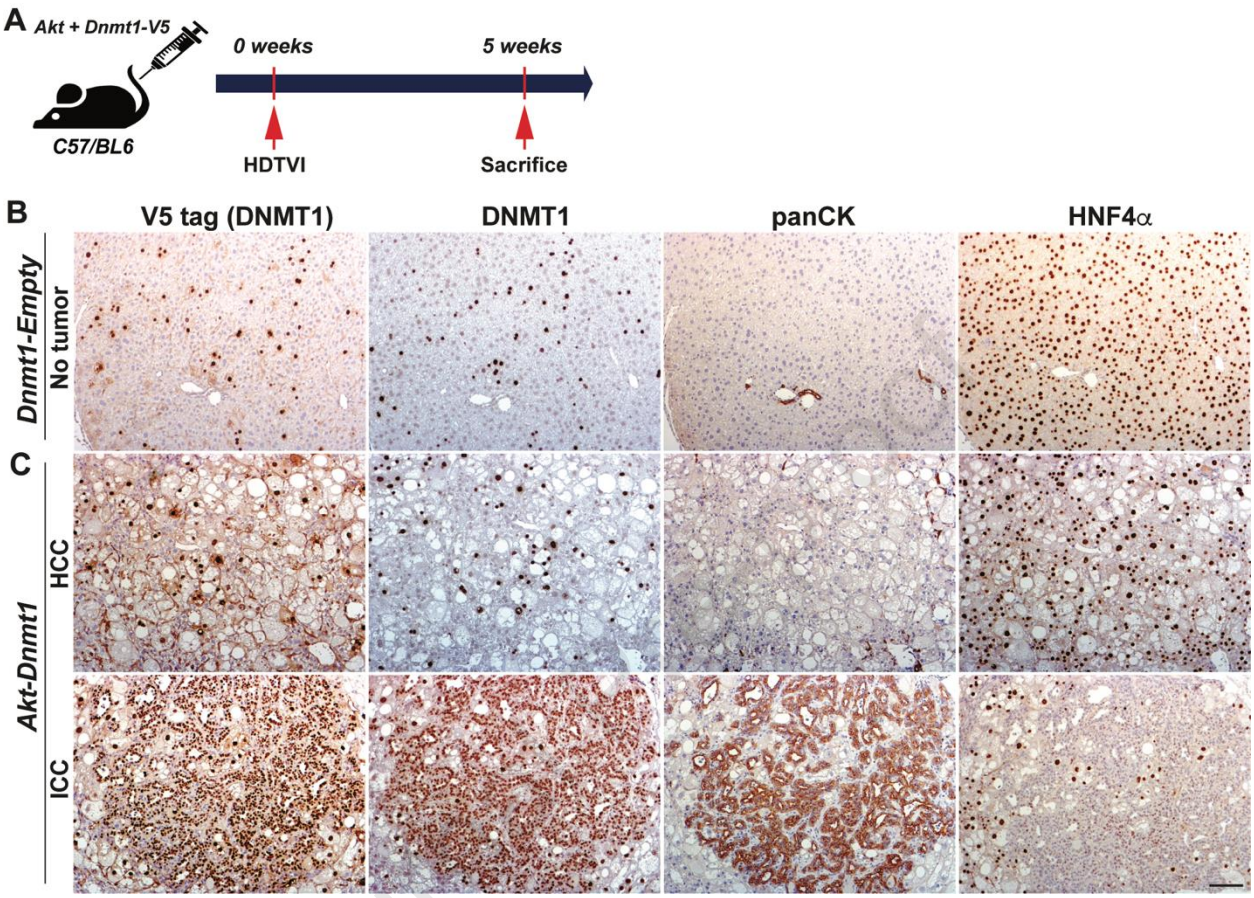

Figure S6: Concomitant expression of *mysAkt* and *Dnmt1* in a subset of murine HCs in vivo induces liver cancer development including ICC. **(A)** Experimental design illustrating plasmids used for HDTVI, mice used in study and time-points analyzed. **(C)** Representative IHC images of 5w *Akt-Dnmt1* show HCC and few ICC components to be positive. **(B)** In *Dnmt1-Empty* liver, no tumor was seen and all V5-tag^{+} cells retained HC morphology without clonal expansion. Scale bars: 100µm.

Figure S7

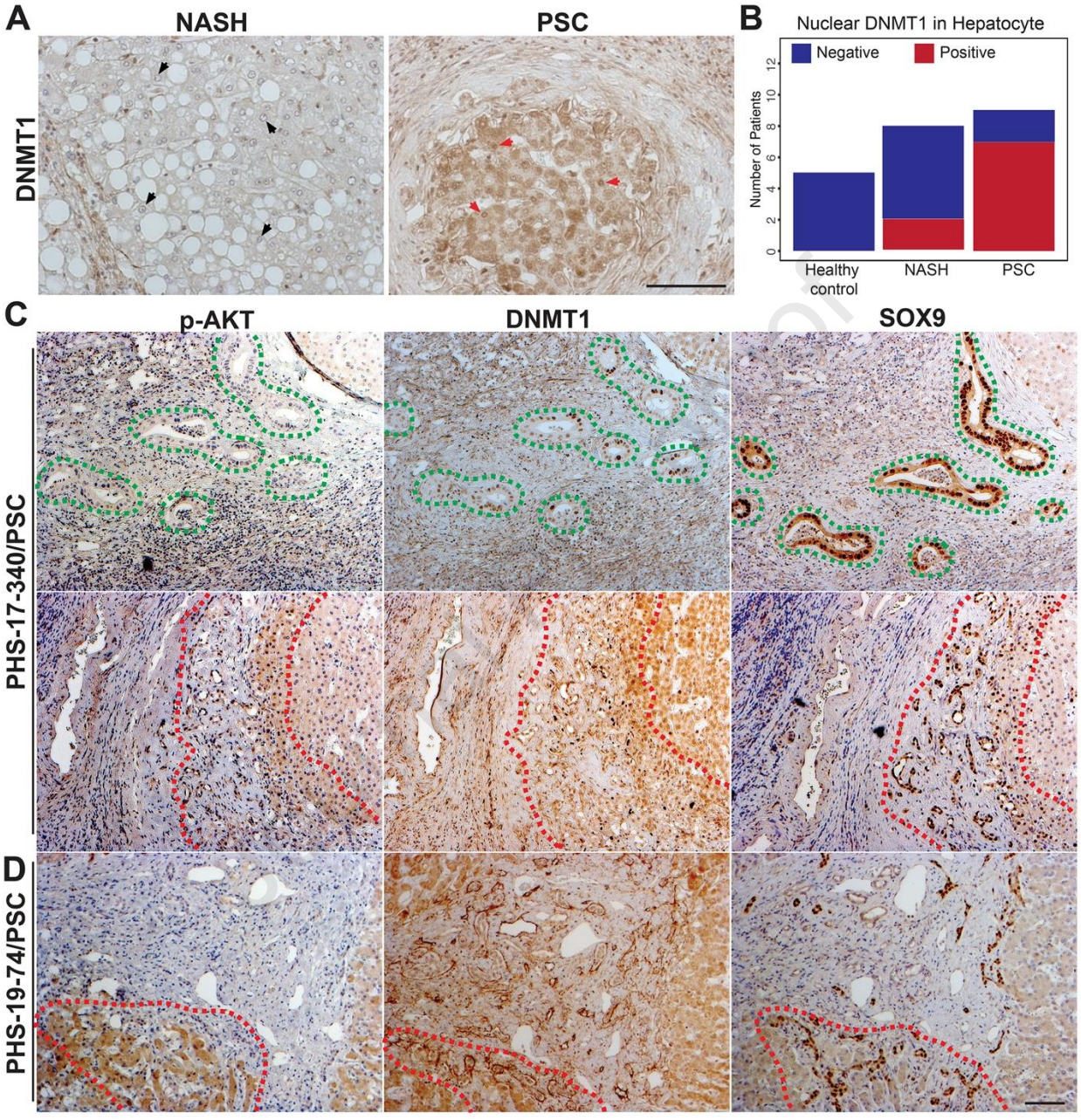

Figure S7. DNMT1 and p-AKT co-expression in PSC cases with ICC-like regions. **(A)** Representative IHC images of liver section from patients with PSC showing increased nuclear DNMT1 in HCs as compared to NASH or healthy liver. Black arrows point to DNMT1^{-} hepatocytes; red arrows to DNMT1^{+} hepatocytes. (**B**) Stacked-bar graph

showing higher incidence of nuclear DNMT1 in HCs in PSC patient livers compared with NASH and healthy livers. **(C and D)** Representative IHC images showing ICC-like premalignant foci in only a subset of PSC patient livers which also showed aberrant expression of p-AKT and DNMT1 in SOX9+ cells. Green dashed lines depicts $SOX9^{+}$;$DNMT1^{+}$;$p\text{-}AKT^{-}$ cells and Red dashed lines depicts $SOX9^{+}$;$DNMT1^{+}$;$p\text{-}AKT^{+}$ cells. Scale bars:100 µm

ONLINE SUPPLEMENT

Table of content:

1. SUPPLEMENTARY METHODS (WITH REFERENCES)

Animal Models of Intrahepatic Cholangiocarcinoma. 10 μg *pT3-EF1α-myrAkt-HA*, 20 μg of *pT3-EF1α-Myc-N1ICD/pT3-EF1α-Flag-YAP1 S127A* and 60 μg mg of *pCMV-Cre (or pCMV-empty)*, or 10 μg *pT3-EF1α-myrAkt-HA* and 20 μg of *pT3-EF1α-Sox9*, or μg mg of *pT3-EF1α-myrAkt-HA-sh-Luciferase*, 20 μg of *pT3-EF1α-Myc-N1ICD, or* 10 μg of *pT3-EF1α-myrAkt-HA-Sh-Yap1*, 20 μg of *pT3-EF1α-Myc-N1ICD*, or 10 μg of *pT3-EF1α-myrAkt-HA-Sh-Dnmt1*, 20 μg of *pT3-EF1α-Myc-N1ICD, or* 10 μg of *pT3-EF1α-myrAkt-HA*, 20 μg of *pT3-EF1α-Myc-N1ICD,* 60 μg *of pT3-EF5α-Dn-TEAD, or* 20 μg of *pT3-EF1α-Myc-N1ICD, 60* μg *of pT3-EF5α-Dn-TEAD, or* 10 μg of *pT3-EF1α-myrAkt-HA-sh-Yap1*, 20 μg of *pT3-EF1α-Myc-N1ICD*, 10 μg and 40 μg of *pT3-EF1α-Dnmt1-V5, or* 10 μg of *pT3-EF1α-myrAkt-HA*, 20 μg of *pT3-EF1α-Myc-N1ICD, 60* μg *of pT3-EF5α-Dn-TEAD, 40* μg *of pT3-EF1α-Dnmt-V5,* or 10 μg of *pT3-EF1α-myrAkt-HA-sh-Luciferase*, 20 μg of *pT3-EF1α-Myc-N1ICD* and 40 μg of *pCMV-empty*, or 10 μg of *pT3-EF1α-myrAkt-HA-sh-Yap1*, 20 μg of *pT3-EF1α-Myc-N1ICD* and 40 μg of *pCMV-Cre*, or 10 μg of *pT3-EF1α-myrAkt-HA*, 20 μg of *Fbxw7ΔF*, or 10 μg of *Kras* G12D, 40 μg of *sh-p53* along with the transposase in a ratio of 25:1 were diluted in 2 ml of normal saline (0.9% NaCl), filtered through 0.22μm filter (Millipore), and hydrodynamically injected into the lateral tail vein of mice[1-3]. All animals were sacrificed between 2-5 weeks of plasmids injections unless otherwise indicated.

Immunohistochemistry (IHC). Mouse liver tissues were fixed for 48 h in 10% neutralized formalin (Fisher Chemicals), transferred into 70% ethanol and then dehydrated and

embedded in paraffin. For IHC, formalin-fixed sections were deparaffinized in graded xylene and ethanol and rinsed in PBS. For antigen retrieval, samples were microwaved for 12 min in pH 6.0 sodium citrate buffer (HA-tag, Myc-tag, panCK, SOX9) or pH 9.0 Tris-EDTA buffer (p-AKT) or DAKO (V5-tag), or were pressure cooked for 20 min in pH 9.0 Tris-EDTA buffer (YAP1 and HNF4α) or were autoclaved for 1 h in pH 9.0 Tris-EDTA buffer (DNMT1). After cooling, samples were placed in 3% H_2O_2 (Fisher Chemicals) for 10 min to quench endogenous peroxide activity. After washing with PBS, slides were blocked with Super Block (ScyTek Laboratories) for 10 min. Sections were incubated for overnight at 4C with the primary antibodies (Supplementary Table 2. Sections were then incubated with species-specific biotinylated secondary antibodies (EMD Millipore, Supplementary Table 2) for 1 h, at room temperature. Sections were incubated with Vectastain ABC Elite kit (Vector Laboratories) and signal was detected with DAB Peroxidase Substrate Kit (Vector Laboratories) followed by quenching in distilled water for 5 min. Slides were counterstained with hematoxylin (ThermoFisher Scientific), dehydrated to xylene (Fisher Chemicals) and coverslips applied with Cytoseal XYL (ThermoFisher Scientific).

Immunofluorescence. Paraffin embedded liver sections (5 μm thick) were deparaffinized using xylene (Fisher Chemicals) and rehydrated by incubating the slices in ethanol (100% and 95% v/v, each 3x5 min) and washed in PBS. Heat-induced epitope retrieval was performed for 20 min using a pressure cooker with pH 6.0 sodium citrate buffer. Sections were washed in PBS, permeabilized for 5 minutes with PBS/0.3% Triton X and blocked with PBS/0.3% Triton X/10% bovine serum albumin (BSA) for 45 minutes

at room temperature. Sections were incubated with primary antibodies in PBS/0.3% Triton X/10% BSA overnight at 4C. At the end of the incubation, sections were washed thrice and incubated with fluorochrome-conjugated secondary antibodies in PBS/0.3% Triton X/10% BSA for 1h at room temperature, then washed in PBS/0.1% Triton X 3 times. Liver sections were mounted using Prolong Gold Antifade w/DAPI (Invitrogen) and pictures were acquired using LSM700 confocal microscope and the Zen Software (Zeiss).

DNMT1 ChIP-seq analysis.

Chromatin Immunoprecipitation: Frozen liver tissue was sent to Active Motif Services (Carlsbad, CA) for ChIP-Seq. Active Motif prepared chromatin, performed ChIP reactions, generated libraries, sequenced the libraries, and performed basic data analysis. In brief, tissue was submersed in PBS + 1% formaldehyde, cut into small pieces, and incubated at room temperature for 15 minutes. Fixation was stopped by the addition of 0.125 M glycine (final). The tissue pieces were then treated with a TissueTearer and finally spun down and washed 2x in PBS. Chromatin was isolated by adding lysis buffer, followed by disruption with a Dounce homogenizer. Lysates were sonicated and the DNA sheared to an average length of 300-500 bp with Active Motif's EpiShear probe sonicator (cat# 53051). Genomic DNA (Input) was prepared by treating aliquots of chromatin with RNase, proteinase K and heat for de-crosslinking, followed by SPRI beads clean up (Beckman Coulter) and quantitation by Clariostar (BMG Labtech). Extrapolation to the original chromatin volume allowed determination of the total chromatin yield. An aliquot of chromatin (40 ug) was precleared with protein A agarose beads (Invitrogen). Genomic DNA regions of interest were isolated using antibodies against DNMT1 (Cell Signaling Technology, cat#:5032). Complexes were washed, eluted from the beads with SDS

buffer, and subjected to RNase and proteinase K treatment. Crosslinks were reversed by incubation overnight at 65C, and ChIP DNA was purified by phenol-chloroform extraction and ethanol precipitation.

ChIP-Sequencing (Illumina): Illumina sequencing libraries (a custom type, using the same paired read adapter oligonucleotides described by Bentley et al., (2008))[4] were prepared from the ChIP and Input DNAs on an automated system (Apollo 342, Wafergen Biosystems/Takara). After a final PCR amplification step, the resulting DNA libraries were quantified and sequenced on Illumina's NextSeq 500 (75 nt reads, single end). Reads were aligned to the mouse genome (mm10) using the BWA algorithm (default settings)[5]. Duplicate reads were removed and only uniquely mapped reads (mapping quality >= 25) were used for further analysis. Alignments were extended in silico at their 3'-ends to a length of 200 bp, which is the average genomic fragment length in the size-selected library, and assigned to 32-nt bins along the genome. The resulting histograms (genomic "signal maps") were stored in bigWig files. Peak locations were determined using the MACS algorithm (v2.1.0) with a cutoff of p-value = 1e-7[6]. Peaks that were on the ENCODE blacklist of known false ChIP-Seq peaks were removed. Signal maps and peak locations were used as input data to Active Motifs proprietary analysis program, which creates Excel tables containing detailed information on sample comparison, peak metrics, peak locations and gene annotations.

REFERENCES

1. Tao J, Zhang R, Singh S, et al. Targeting beta-catenin in hepatocellular cancers induced by coexpression of mutant beta-catenin and K-Ras in mice. Hepatology 2017;65:1581-1599.
2. Fan B, Malato Y, Calvisi DF, et al. Cholangiocarcinomas can originate from hepatocytes in mice. J Clin Invest 2012;122:2911-5.

3. Wang J, Dong M, Xu Z, et al. Notch2 controls hepatocyte-derived cholangiocarcinoma formation in mice. Oncogene 2018;37:3229-3242.
4. Bentley DR, Balasubramanian S, Swerdlow HP, et al. Accurate whole human genome sequencing using reversible terminator chemistry. Nature 2008;456:53-9.
5. Li H, Durbin R. Fast and accurate short read alignment with Burrows-Wheeler transform. Bioinformatics 2009;25:1754-60.
6. Zhang Y, Liu T, Meyer CA, et al. Model-based analysis of ChIP-Seq (MACS). Genome Biol 2008;9:R137.

2. SUPPLEMENTARY TABLES

Table S1: Summary of Patients with PSC and NASH used in the study.

Patient Record Number	Age	Sex	SOX9	pAKT S473	YAP	Hepatocyte DNMT1		Disease
						C	N	
PHR17-187	44	F	<20%	NEG	20-50%	100%	NEG	PSC
PHR17-315	39	M	NEG	NEG	<20%	100%	NEG	PSC
PHR17-318	32	M	20-50%	NEG	<20%	50%	20-50%	PSC
PHR17-340	47	F	20-50%	<20%	20-50%	100%	20-50%	PSC
PHR17-471	44	F	<20%	<20%	NEG	100%	<20%	PSC
PHS18-35	35	M	<20%	<20%	NEG	0%	NEG	PSC
PHR19-64	24	M	<20%	20-50%	20-50%	100%	<20%	PSC
PHR19-67	32	F	NEG	NEG	<20%			PSC
PHR19-74	50	M	<20%	20-50%	<20%	100%	<20%	PSC
PHR19-80	61	F	NEG	20-50%	<20%	100%	NEG	PSC
PHR16-107	67	M	<20%	<20%	<20%	0%	0	NASH
PHR17-50	73	F	<20%	NEG	<20%	0%	NEG	NASH
PHR17-114	53	F	20-50%	20-50%	NEG			NASH
PHR17-235	63	M	20-50%	20-50%	NEG	0%	NEG	NASH
PHR17-238	65	M	<20%	20-50%	NEG	50%	NEG	NASH
PHR17-247	61	M	<20%	NEG	<20%			NASH
PHR17-299	56	F	<20%	<20%	<20%	<20%	0	NASH
PHR18-25	68	F	20-50%	20-50%	<20%	50%	<20%	NASH
PHR18-219	62	F	<20%	NEG	<20%	<20%	<20%	NASH
PHR19-107	78	F	<20%	<20%	<20%	100%	NEG	NASH
NHL1029			NEG	NA	NEG			Healthy control liver
16-5566	54	F	NEG	NEG	NEG			Healthy control liver (underlying colon adenocarcinoma)
12-9718	60	M	NEG	NEG	NEG			Healthy control liver (underlying colon adenocarcinoma)

17-9693	49	F	NEG	NEG	NEG			Healthy control liver (underlying colon adenocarcinoma)
13-15397	54	F	NEG	NEG	20-50%			Healthy control liver (underlying colon adenocarcinoma)
14-2191	36	M	NEG	NEG	NEG			Healthy control liver (underlying colon adenocarcinoma)
PHS18-34295						0	NEG	Healthy control liver
PHS18-11592						0	NEG	Healthy control liver
PHS18-5904						0	NEG	Healthy control liver
PHS16-40535						0	NEG	Healthy control liver
PHS16-32066						0	NEG	Healthy control liver

Abbreviations: C-cytoplasmic; **N-** nuclear; **PSC-** Primary sclerosing cholangitis; **NASH-** Non alcoholic steatohepatitis

Table S2: Antibody List used in the study

Primary Antibodies:

Target	Species	Dilution	Source	Catalog Number
HA-tag	Mouse	1:50 (IHC)	Cell Signaling	CS2367
MYC-tag	Rabbit	1:100 (IHC)	Maine Medical Center Research Institute (mmcri)	Vli01
Pan-CYTOKERATIN (panCK)	Rabbit	1:200 (IHC)	Dako	Z0622
p-AKT	Rabbit	1:100 (IHC)	Cell Signaling	CS4060
SOX9	Rabbit	1:200 (IF) 1:2000 (IHC)	EMD Millipore	Ab5535
YAP1	Rabbit	1:100 (IF and IHC)	Cell Signaling	CS14074
HNF4α	Rabbit	1:100 (IHC)	Cell Signaling	CS3113
PCNA	Mouse	1:200 (IF)	Santa Cruz	sc-56
CK19	Rat	1:10 (IF)	DSHB	TROMA III
DNMT1	Rabbit	1:100 (IHC)	Abcam	ab188453

Secondary Antibodies:

Secondary Antibody	Species	Source	Catalog Number
Donkey anti-Rabbit IgG Biotin	Donkey	EMD Millipore	AP182B
Goat anti-Mouse IgG (H+L) Biotin	Goat	EMD Millipore	AP181B
Alexa-Fluor 555 Donkey anti-Rabbit IgG (H+L)	Donkey	Invitrogen	A31572
Alexa-Fluor 488 Donkey anti-Rat IgG (H+L)	Donkey	Invitrogen	A21208
Alexa-Fluor 647 Goat anti-Mouse IgG (H+L)	Goat	Invitrogen	A21236

Table S3: List of 200 genes used to estimate the genetic identity of *Akt-NICD*-ICC transcriptome with large clinical ICC cohort by Nearest Template Prediction assay

Number	Gene
1	TAGLN2
2	COL4A1
3	SPP1
4	CCND1
5	COL4A2
6	NRARP
7	ENC1
8	OSMR
9	KRT8
10	MKI67
11	ANXA2
12	ADCY5
13	PXDN
14	PODXL
15	TRIM47
16	DDR1
17	SOX9
18	SPON1
19	LBH
20	FSTL1
21	ANXA5
22	TPM4
23	SOX4
24	FLNA
25	B4GALT6
26	ELN
27	S100A11
28	ARL4C
29	CELSR2
30	KRT18
31	CD9

32	VCAM1
33	SLCO3A1
34	ADAMTS1
35	LAMA5
36	TUBA1A
37	CSRP1
38	TOP2A
39	FAR1
40	FADS3
41	EIF2AK3
42	TRIB2
43	SYNPO
44	DCDC2
45	TTYH1
46	CD63
47	DKK3
48	FAM118A
49	SH3PXD2B
50	JAG1
51	CLASP1
52	PTPN13
53	VIM
54	TGM2
55	EHF
56	PTK7
57	SCARA3
58	BCAM
59	BICC1
60	CKB
61	LMNA
62	PRC1
63	MARCKS
64	MCAM
65	BMP6
66	ENAH
67	STMN1
68	PFKFB4
69	RHBDF1
70	MAP1B

71	ADGRG1
72	SRC
73	MAP2
74	ANLN
75	VILL
76	HEYL
77	WLS
78	SMTNL2
79	GAS6
80	ELF3
81	ACTN1
82	PHLDA3
83	CENPF
84	PPP1R9B
85	MGAT5
86	GPC6
87	SERPINB6
88	ARHGEF10
89	VSIG10
90	COL1A1
91	GLS
92	ZNF703
93	AGPAT1
94	RACGAP1
95	CDKN1A
96	CDH15
97	SCD
98	LIG1
99	LTBP1
100	INHBB
101	CELA1
102	CYP4F12
103	FAM210A
104	CYP2D6
105	CDC14B
106	GNA12
107	RNF103
108	FECH
109	SUCNR1

110	AK3
111	IPMK
112	SULT1B1
113	PDK2
114	RETSAT
115	FBXO8
116	STAT5B
117	CAT
118	ERBB3
119	SLC25A42
120	SFXN5
121	PGM2
122	C16orf70
123	MN1
124	TYMP
125	GNS
126	CHUK
127	DHRS3
128	CMBL
129	TSC1
130	SELENBP1
131	RNF152
132	MOCS1
133	ABCD3
134	NFIX
135	SLC2A2
136	NDST1
137	RMND5A
138	CHPT1
139	FOXN3
140	ETFDH
141	HLF
142	GGACT
143	DYRK2
144	AL049629.2
145	ABCG8
146	IDH3B
147	HSD17B11
148	PXMP4

149	AGTR1
150	HSD11B1
151	INSIG2
152	KHNYN
153	ZCCHC24
154	CA1
155	PNPLA8
156	SNX29
157	CYB5R3
158	ALDH5A1
159	SDR42E1
160	NQO2
161	ACBD5
162	KHK
163	OPA1
164	DONSON
165	NAA60
166	TSPAN12
167	NPC1
168	FTCD
169	SEPHS2
170	UQCRB
171	ZFAND6
172	SCAP
173	PTTG1IP
174	MCC
175	PCTP
176	CYP4F8
177	RUFY3
178	ECM1
179	PRKD3
180	PPARGC1B
181	SASH1
182	DENND4A
183	FAM13A
184	HMGCS2
185	HYKK
186	SDHC
187	CA14

188	ACOT12
189	RILP
190	UGT1A1
191	CLDN1
192	NR1H4
193	ISOC1
194	NDUFA10
195	ACSL1
196	PAQR7
197	RNF125
198	PBLD
199	SLC6A9
200	MLXIPL

Table S4: List of 169 overlapped genes by integration of DNMT1 ChIP-seq and down-regulated in transcriptome profile

Number	Gene
1	GM4980
2	DENND4A
3	ACAD11
4	INCA1
5	ARRDC3
6	PTTG1IP
7	SMIM13
8	ACO1
9	AK2
10	APBA2
11	ATP5A1
12	ZFP36L1
13	C2
14	CHUK
15	PLK3
16	COX5A
17	CREM
18	CYP26A1
19	DCT
20	DYRK1B
21	EFNA3
22	EVI5
23	F8
24	FTL1
25	GAS1
26	GATA4
27	GCGR
28	GCH1
29	GOT2
30	AES
31	H2-KE6
32	FOXQ1
33	HHEX
34	HLX

35	IGFBP4
36	INSR
37	IRS1
38	MAFB
39	LHX2
40	ELOVL6
41	SLC8B1
42	AMACR
43	CRELD1
44	NPAS2
45	NPC1
46	NUMB
47	P2RY2
48	PDE9A
49	PITX3
50	RORA
51	SEMA6C
52	SOD1
53	CAMKK2
54	SLC25A38
55	SNED1
56	SDC4
57	SPRN
58	SH3BGRL2
59	ALDH4A1
60	SLC6A6
61	CECR5
62	TCP11L2
63	UGP2
64	GLTPD2
65	L2HGDH
66	VWA8
67	DLGAP1
68	LIMS2
69	ZADH2
70	ATRNL1
71	RNF103
72	C130074G19RIK
73	ZFP36

74	SLC25A25
75	PDK1
76	NUDT6
77	CREBL2
78	TUFM
79	ZBTB44
80	SH3BP5
81	GABBR2
82	GPRIN3
83	BAHCC1
84	GPHN
85	GPR157
86	BC024139
87	SLC25A10
88	MRPL39
89	ABCA8B
90	ABCC6
91	MARVELD1
92	ULK2
93	VPS13C
94	SLC35E2
95	DENND5B
96	ATP11C
97	MIA3
98	NR1D2
99	TLCD2
100	RBM33
101	DRC1
102	PDP2
103	CREG1
104	MN1
105	SHF
106	LRP3
107	SLC25A13
108	TNK2
109	ACAA2
110	GNPNAT1
111	EPB4.1L4B
112	ABCB10

113	NGLY1
114	GM6484
115	TSC1
116	ASB2
117	EEFSEC
118	ABHD6
119	1110001J03RIK
120	AAED1
121	NDUFB9
122	PYURF
123	FIGNL2
124	HINT3
125	ACADSB
126	LONP2
127	PXDC1
128	NDUFA6
129	PNPLA8
130	MMD
131	EEPD1
132	RNF125
133	DGAT2
134	ATG101
135	GCSH
136	0610030E20RIK
137	PCYT2
138	ELOVL5
139	DDAH1
140	HIST1H4H
141	CHN2
142	MPC2
143	MIPEP
144	CABYR
145	ARHGAP42
146	AMDHD1
147	PITPNC1
148	OSGIN1
149	LRPPRC
150	MBLAC2
151	PMPCB

152	SLC25A16
153	RHOX13
154	NMNAT3
155	GBE1
156	TBC1D30
157	TBC1D30
158	ARL5A
159	1700001C19RIK
160	FGGY
161	KLHL24
162	DOCK8
163	GRHPR
164	MND1
165	OCEL1
166	9430038I01RIK
167	CML2
168	PHLPP1
169	RDH10

Table S5: 320 upstream regulators for identified 169 overlapped genes (Table S4) predicted by IPA-URA tool

Upstream Regulator	Molecule Type	p-value of overlap
methylprednisolone	chemical drug	4.36E-07
INSR	kinase	7.17E-06
moxonidine	chemical drug	1.07E-04
CPT1B	enzyme	1.15E-04
mono-(2-ethylhexyl)phthalate	chemical toxicant	1.37E-04
D-glucose	chemical - endogenous mammalian	1.98E-04
IGF2BP2	translation regulator	2.75E-04
ANGPTL7	other	2.75E-04
methotrexate	chemical drug	3.22E-04
peoniflorin	chemical drug	3.27E-04
APP	other	3.71E-04
TP53	transcription regulator	4.07E-04
SMYD1	transcription regulator	4.71E-04
tert-butyl-hydroquinone	chemical reagent	4.91E-04
LONP1	peptidase	5.15E-04
PTPN1	phosphatase	5.43E-04
isobutylmethylxanthine	chemical toxicant	7.65E-04
NKX2-2-AS1	other	8.09E-04
USP28	peptidase	9.51E-04
LDHB	enzyme	9.51E-04
ABCB7	transporter	9.51E-04
INS	other	9.93E-04
metribolone	chemical reagent	1.03E-03
IGF2	growth factor	1.12E-03
CEBPA	transcription regulator	1.19E-03
DIO3	enzyme	1.23E-03
Ck2	complex	1.62E-03
IGF2R	transmembrane receptor	2.01E-03
CLOCK	transcription regulator	2.06E-03

GRB10	other	2.45E-03
sphingomyelin	chemical - endogenous mammalian	2.45E-03
GCG	other	2.53E-03
PNPLA2	enzyme	2.64E-03
beraprost	chemical drug	2.92E-03
NFU1	other	2.95E-03
NUPR1	transcription regulator	2.98E-03
WNT3A	cytokine	3.00E-03
UQCC3	other	3.12E-03
GNAQ	enzyme	3.51E-03
beta-carotene	chemical - endogenous mammalian	3.59E-03
streptozocin	chemical drug	3.78E-03
elaidic acid	chemical - endogenous mammalian	3.81E-03
pirinixic acid	chemical toxicant	3.96E-03
Cd2+	chemical toxicant	3.99E-03
DSCAM	other	4.11E-03
FFAR4	G-protein coupled receptor	4.59E-03
CG	complex	5.37E-03
topiramate	chemical drug	5.69E-03
PRKAG3	kinase	5.70E-03
miR-124-3p (and other miRNAs w/seed AAGGCAC)	mature microRNA	5.84E-03
TO-901317	chemical reagent	6.20E-03
leukotriene D4	chemical - endogenous mammalian	6.31E-03
HNF1A	transcription regulator	6.46E-03
raloxifene	chemical drug	6.60E-03
IGFBP2	other	6.64E-03
rosiglitazone	chemical drug	6.80E-03
RDH5	enzyme	6.83E-03
KLHL13	other	6.83E-03
KLHL9	other	6.83E-03
Gm13570/Gm4984	other	6.83E-03
JAKMIP1	other	6.83E-03

PISD	enzyme	6.83E-03
GRB14	other	6.83E-03
SNX5	transporter	6.83E-03
M6PR	transporter	6.83E-03
FAM13A	other	6.83E-03
diacetylbis(4-methylthiosemicarbazonato)copper(II)	chemical reagent	6.83E-03
MID-1	chemical reagent	6.83E-03
myrcene	chemical - endogenous non-mammalian	6.83E-03
cineole	chemical drug	6.83E-03
FOXA2	transcription regulator	6.83E-03
dexamethasone	chemical drug	6.93E-03
ZC3H12A	enzyme	7.09E-03
LEP	growth factor	7.33E-03
PHLPP1	enzyme	7.34E-03
DBP	transcription regulator	7.34E-03
GSK3A	kinase	7.34E-03
PRKCG	kinase	7.67E-03
RPA1	other	8.12E-03
POR	enzyme	8.14E-03
GnRH analog	biologic drug	8.17E-03
Esrra	transcription regulator	8.28E-03
HOXA9	transcription regulator	8.33E-03
IGF1	growth factor	8.48E-03
MAP4K4	kinase	8.78E-03
MECP2	transcription regulator	9.29E-03
PLN	transporter	9.59E-03
TRIM2	enzyme	9.78E-03
fenofibrate	chemical drug	1.04E-02
sirolimus	chemical drug	1.06E-02
TSPYL5	other	1.07E-02
MGP	other	1.07E-02
SULT1E1	enzyme	1.07E-02
diallyl trisulfide	chemical - endogenous non-mammalian	1.07E-02

BACH1	transcription regulator	1.09E-02
IL4	cytokine	1.09E-02
cyclic AMP	chemical - endogenous mammalian	1.09E-02
tributyltin	chemical reagent	1.13E-02
TINCR	other	1.16E-02
Z-LLL-CHO	chemical - protease inhibitor	1.18E-02
ESR2	ligand-dependent nuclear receptor	1.20E-02
mir-133	microRNA	1.22E-02
HNF4A	transcription regulator	1.24E-02
CD3	complex	1.25E-02
COMMD1	transporter	1.25E-02
IRS1	enzyme	1.29E-02
GNA14	enzyme	1.32E-02
CD 437	chemical drug	1.34E-02
ACLY	enzyme	1.35E-02
SRD5A1	enzyme	1.35E-02
SD 0006	chemical reagent	1.36E-02
LINC00667	other	1.36E-02
STARD4	transporter	1.36E-02
SOCS7	other	1.36E-02
USP46	peptidase	1.36E-02
PTPase	group	1.36E-02
TCDD-AHR	complex	1.36E-02
FBXW8	enzyme	1.36E-02
beta-apo-14'-carotenal	chemical - endogenous mammalian	1.36E-02
NKIRAS1	enzyme	1.36E-02
ME1	enzyme	1.36E-02
GABRG2	ion channel	1.36E-02
DNAJB1	transcription regulator	1.36E-02
bavachalcone	chemical reagent	1.36E-02
primaquine	chemical drug	1.36E-02
milrinone	chemical drug	1.36E-02
talarozole	chemical drug	1.36E-02

glipizide	chemical drug	1.36E-02
apo-13-lycopenone	chemical reagent	1.36E-02
apo-15-lycopenal	chemical reagent	1.36E-02
ZBTB7B	transcription regulator	1.37E-02
CD300LF	other	1.45E-02
NR4A1	ligand-dependent nuclear receptor	1.57E-02
miR-223-3p (miRNAs w/seed GUCAGUU)	mature microRNA	1.67E-02
CCL5	cytokine	1.69E-02
miR-7a-5p (and other miRNAs w/seed GGAAGAC)	mature microRNA	1.78E-02
N(G)-monomethyl-D-arginine	chemical - endogenous mammalian	1.78E-02
FOXO1	transcription regulator	1.79E-02
IFRD1	other	1.89E-02
PSEN1	peptidase	1.95E-02
beta-estradiol	chemical - endogenous mammalian	1.97E-02
ALDH1A2	enzyme	2.01E-02
NCOA4	transcription regulator	2.01E-02
IRS	group	2.03E-02
TAF3	transcription regulator	2.03E-02
DNAJA2	enzyme	2.03E-02
STARD5	transporter	2.03E-02
dapagliflozin	chemical drug	2.03E-02
PHYH	enzyme	2.03E-02
aurora kinase inhibitor III	chemical - kinase inhibitor	2.03E-02
FTMT	enzyme	2.03E-02
AFDN	other	2.03E-02
NEU1	enzyme	2.03E-02
RDH16	enzyme	2.03E-02
BRF110	chemical reagent	2.03E-02
CDD450	chemical drug	2.03E-02
actinomycin	chemical - endogenous non-mammalian	2.03E-02
quinine	chemical drug	2.03E-02

glyphosate	chemical toxicant	2.03E-02
TLE3	other	2.11E-02
AHCY	enzyme	2.13E-02
SCAP	other	2.24E-02
cinnamaldehyde	chemical toxicant	2.24E-02
bardoxolone	chemical drug	2.25E-02
Insulin	group	2.27E-02
PTGER4	G-protein coupled receptor	2.28E-02
RYR1	ion channel	2.38E-02
CA9	enzyme	2.38E-02
daunorubicin	chemical drug	2.38E-02
TRAP1	enzyme	2.45E-02
CD38	enzyme	2.47E-02
Stat3-Stat3	complex	2.51E-02
CEBPB	transcription regulator	2.51E-02
hydrocortisone	chemical - endogenous mammalian	2.52E-02
EGLN	group	2.52E-02
ST1926	chemical drug	2.52E-02
TSC2	other	2.57E-02
Hbb-b1	transporter	2.59E-02
GNB2	enzyme	2.64E-02
nicotinic acid	chemical - endogenous mammalian	2.64E-02
RARG	ligand-dependent nuclear receptor	2.66E-02
SKA3	other	2.70E-02
GPR55	G-protein coupled receptor	2.70E-02
tyrosine kinase	group	2.70E-02
MCU	ion channel	2.70E-02
CCDC3	other	2.70E-02
FDX2	transporter	2.70E-02
OPN3	G-protein coupled receptor	2.70E-02
MITF-p300/CBP	complex	2.70E-02
PX 478	chemical drug	2.70E-02
GH2	other	2.70E-02

FGD5-AS1	other	2.70E-02
mir-32	microRNA	2.70E-02
FDXR	enzyme	2.70E-02
HAP1	other	2.70E-02
AK4	kinase	2.70E-02
diamide	chemical reagent	2.70E-02
9-cis-retinal	chemical - endogenous mammalian	2.70E-02
thymeleatoxin	chemical toxicant	2.70E-02
MBTD1	other	2.77E-02
Immunoglobulin	complex	2.78E-02
DYSF	other	2.81E-02
methamphetamine	chemical drug	2.81E-02
lipopolysaccharide	chemical drug	2.88E-02
PRKN	enzyme	2.89E-02
HDL-cholesterol	complex	2.91E-02
CARM1	transcription regulator	2.91E-02
GNB1	enzyme	2.91E-02
BTG2	transcription regulator	2.91E-02
sucrose	chemical - endogenous mammalian	2.91E-02
HDAC3	transcription regulator	3.04E-02
ATP7B	transporter	3.05E-02
CTF1	cytokine	3.05E-02
GLI1	transcription regulator	3.14E-02
SAMMSON	other	3.19E-02
M344	chemical reagent	3.19E-02
dihydrotestosterone	chemical - endogenous mammalian	3.27E-02
N-nitro-L-arginine methyl ester	chemical drug	3.28E-02
propofol	chemical drug	3.34E-02
PAX5-ELN	fusion gene/product	3.34E-02
S-nitrosoglutathione	chemical toxicant	3.34E-02
PSEN2	peptidase	3.36E-02
inositol	chemical drug	3.37E-02
ginsenoside Re	chemical drug	3.37E-02

ZC3H10	other	3.37E-02
MPC1	transporter	3.37E-02
ALDH3A2	enzyme	3.37E-02
insulin detemir	biologic drug	3.37E-02
miR-202-3p (and other miRNAs w/seed GAGGUAU)	mature microRNA	3.37E-02
mir-191	microRNA	3.37E-02
BCAR3	other	3.37E-02
tofogliflozin	chemical drug	3.37E-02
Meis1	transcription regulator	3.37E-02
mini-GAGR	chemical reagent	3.37E-02
CB-PIC	chemical reagent	3.37E-02
chlorine	chemical toxicant	3.37E-02
SLC27A2	transporter	3.48E-02
pituitary adenylate cyclase-activating polypeptide	biologic drug	3.48E-02
NGF	growth factor	3.56E-02
trans-hydroxytamoxifen	chemical drug	3.57E-02
PPARGC1A	transcription regulator	3.59E-02
ethanol	chemical - endogenous mammalian	3.62E-02
HBA1/HBA2	transporter	3.63E-02
LRP5	transmembrane receptor	3.63E-02
ESRRB	transcription regulator	3.79E-02
thyroid hormone	chemical - endogenous mammalian	3.82E-02
uranyl nitrate	chemical toxicant	3.88E-02
HNRNPH1	other	3.94E-02
CUL4B	other	3.94E-02
NFIB	transcription regulator	3.94E-02
bafilomycin A1	chemical drug	3.94E-02
MTOR	kinase	3.96E-02
SERCA	group	4.03E-02
Cbp/p300-Maf-Nfe2l2	complex	4.03E-02
PGRMC2	transporter	4.03E-02
VANGL2	other	4.03E-02

GSK690693	chemical drug	4.03E-02
KCNIP2	transporter	4.03E-02
miR-137-3p (miRNAs w/seed UAUUGCU)	mature microRNA	4.03E-02
SRPK1	kinase	4.03E-02
NOCT	transcription regulator	4.03E-02
CAMK1	kinase	4.03E-02
BARD1	transcription regulator	4.03E-02
zonisamide	chemical drug	4.03E-02
GSK2837808A	chemical reagent	4.03E-02
Z-Leu-Leu-Leu-B(OH)2	chemical reagent	4.03E-02
methyllycaconitine	chemical toxicant	4.03E-02
N-retinylidene-N-retinylethanolamine	chemical - endogenous mammalian	4.03E-02
2,4,5,2',4',5'-hexachlorobiphenyl	chemical toxicant	4.06E-02
IRF4	transcription regulator	4.08E-02
topotecan	chemical drug	4.08E-02
doxorubicin	chemical drug	4.12E-02
palmitic acid	chemical - endogenous mammalian	4.17E-02
SCD	enzyme	4.22E-02
H2AX	transcription regulator	4.26E-02
ADRA1B	G-protein coupled receptor	4.26E-02
ADRA1D	G-protein coupled receptor	4.26E-02
n-3 fatty acids	chemical drug	4.26E-02
SREBF1	transcription regulator	4.28E-02
Rxr	group	4.33E-02
SPARC	other	4.33E-02
miR-1-3p (and other miRNAs w/seed GGAAUGU)	mature microRNA	4.35E-02
PAF1	other	4.42E-02
PDX1	transcription regulator	4.49E-02
ONECUT1	transcription regulator	4.50E-02
Hedgehog	group	4.58E-02
ZNF100	transcription regulator	4.68E-02
ZNF85	transcription regulator	4.68E-02

ZNF254	transcription regulator	4.68E-02
RASSF8	other	4.68E-02
ZNF431	transcription regulator	4.68E-02
USP29	peptidase	4.68E-02
ACIN1	enzyme	4.68E-02
PDE6B	enzyme	4.68E-02
COMT	enzyme	4.68E-02
RHEB	enzyme	4.68E-02
PDE3A	enzyme	4.68E-02
ZNF665	other	4.68E-02
ZNF528	other	4.68E-02
HOXC-AS3	other	4.68E-02
ZNF43	transcription regulator	4.68E-02
ZNF429	transcription regulator	4.68E-02
SORL1	transporter	4.68E-02
SENP2	peptidase	4.68E-02
GNMT	enzyme	4.68E-02
ZNF708	other	4.68E-02
thenoyltrifluoroacetone	chemical reagent	4.68E-02
HI-TOPK32	chemical reagent	4.68E-02
RORC	ligand-dependent nuclear receptor	4.71E-02
RICTOR	other	4.79E-02
IL5	cytokine	4.91E-02
inosine	chemical - endogenous mammalian	4.92E-02
MAP2K5	kinase	4.92E-02
ADRA1A	G-protein coupled receptor	4.92E-02
CTBP1	enzyme	4.92E-02
cisplatin	chemical drug	4.93E-02
KMT2D	transcription regulator	5.00E-02
quercetin	chemical drug	7.22E-02
acetaminophen	chemical drug	8.35E-02

3. Supplementary Figures and Legends

Figure S1

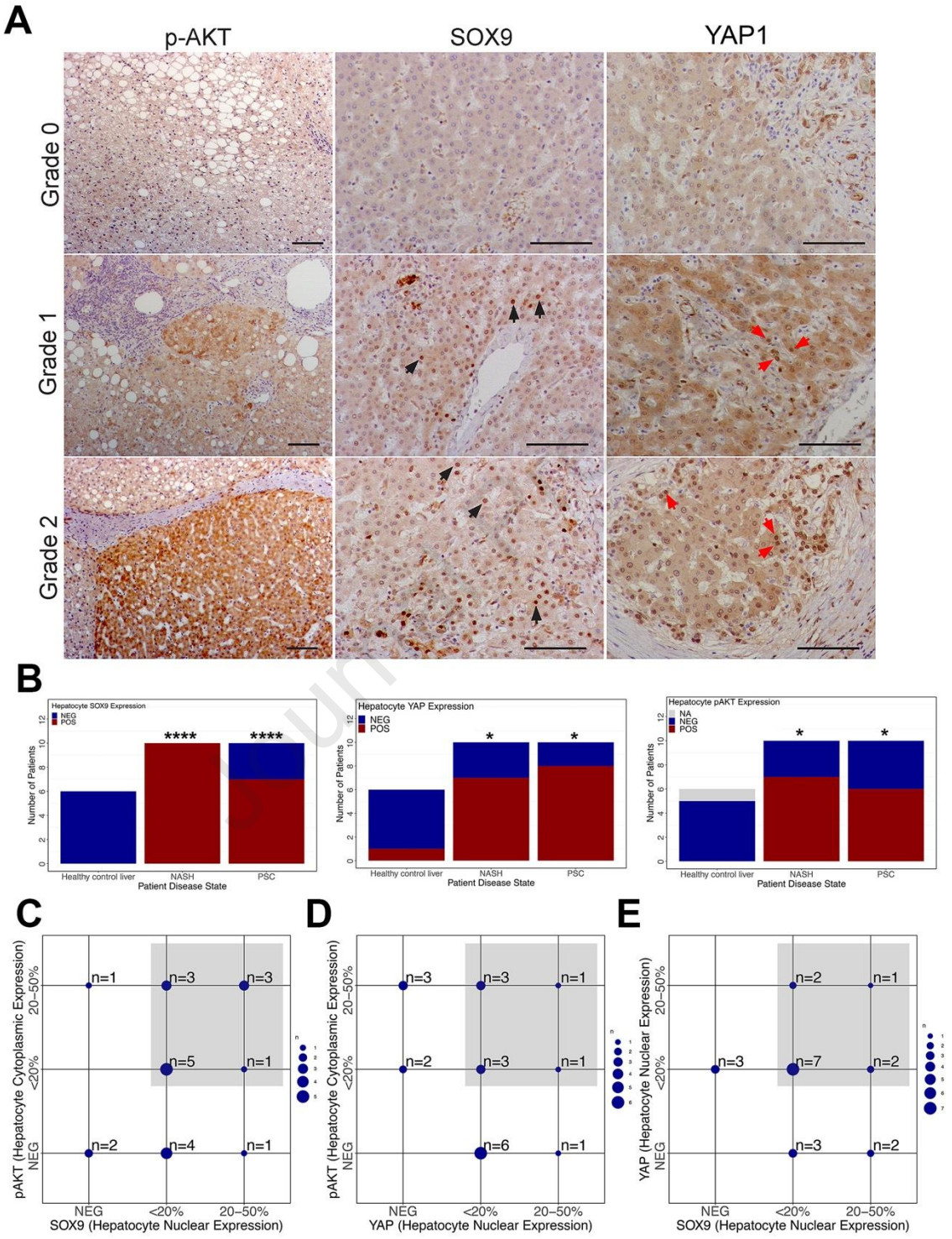

Figure S1. Activation of p-AKT, YAP1 and SOX9 in human liver diseases with higher risk for the development of ICC. (**A**) Representative human liver section images used for arbitrary scoring for p-AKT, SOX9 and YAP1 expression by IHC. Grade 0, no expression; grade 1< 20%; grade 2<50% (Grade 1 and 2 are considered positive). (**B)** Comparison of the number of patients with positive expression of SOX9, YAP1, or p-AKT in HCs shows an enrichment in positive HCs among PSC and NASH patients vs healthy controls. **(C-E)** Overlap in the expression of YAP1, SOX9, and p-AKT among patients with PSC and NASH shows most patients have at least 2 of 3 markers upregulated. Scale bars:100 µm. *p<0.05; ****p< 0.0001.

Figure S2

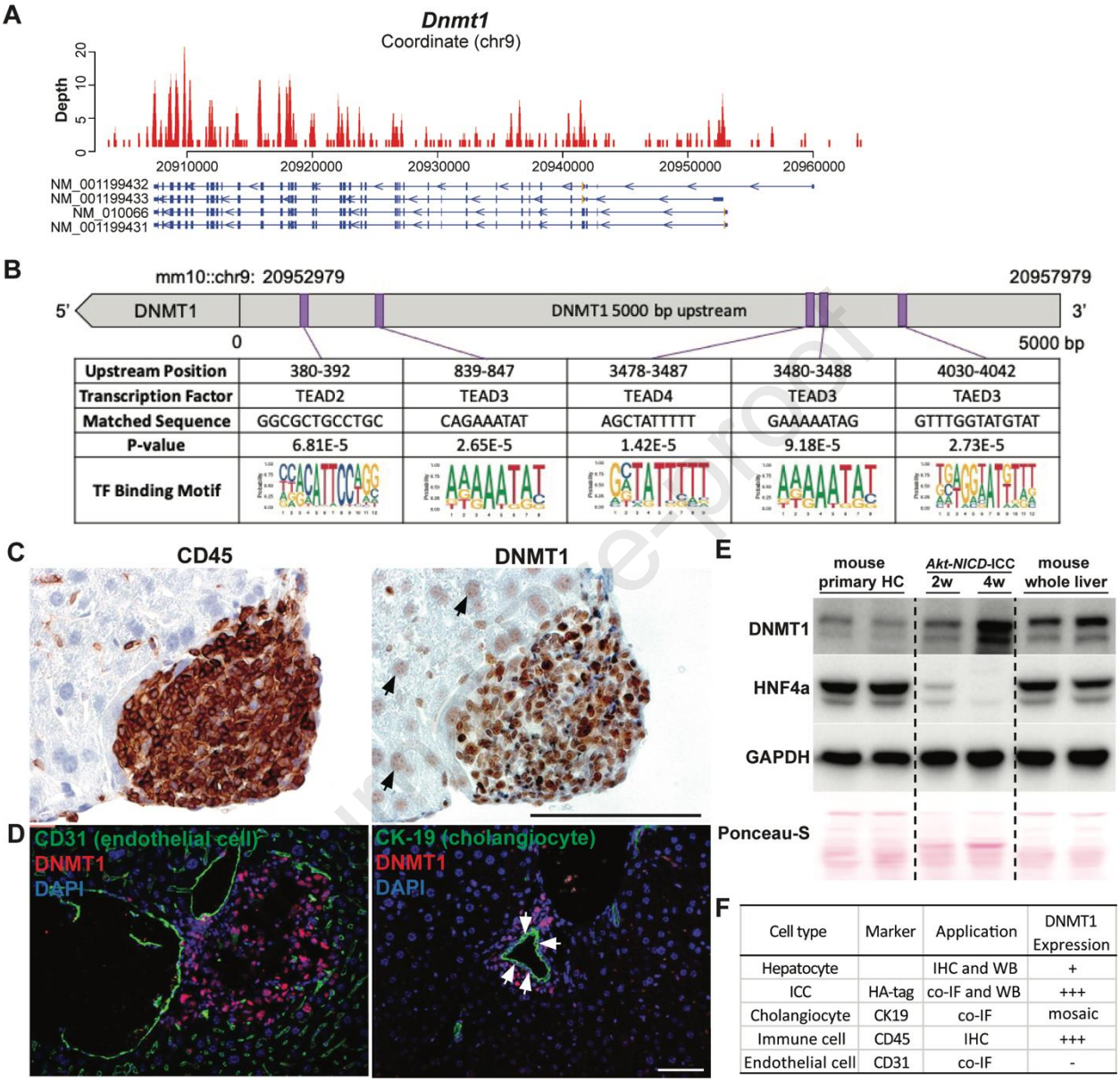

Figure S2. DNMT1 expression in mouse liver. (A) ChIP-seq data for TEAD4 binding sites on *Dnmt1* genomic regions are collected form GEO GSM2882182. **(B)** Predicted TEAD2/TEAD3/TEAD4 binding sites located at 5,000 bp upstream from *Dnmt1* transcription start site. **(C)** IHC staining for *Akt-NICD* KO ICC liver at 5 weeks post HDTVI showing strong DNMT1 expression in $CD45^{+}$ immune cells whereas weak expression in HCs (arrows). **(D)** Co-IF showing strong nuclear DNMT1 expression in

subset of CK-19+ cholangiocytes but not in CD31+ endothelial cells in the liver. **(E)** Representative WB from two independent experiment shows weak DNMT1 expression in HNF4a-enriched mouse primary HCs while strong augment of DNMT1 during transformation into ICC cells. **(F)** Table summarizing the DNMT1 expression pattern in diverse cell types in the liver. scale bar: 100 um.

Figure S3

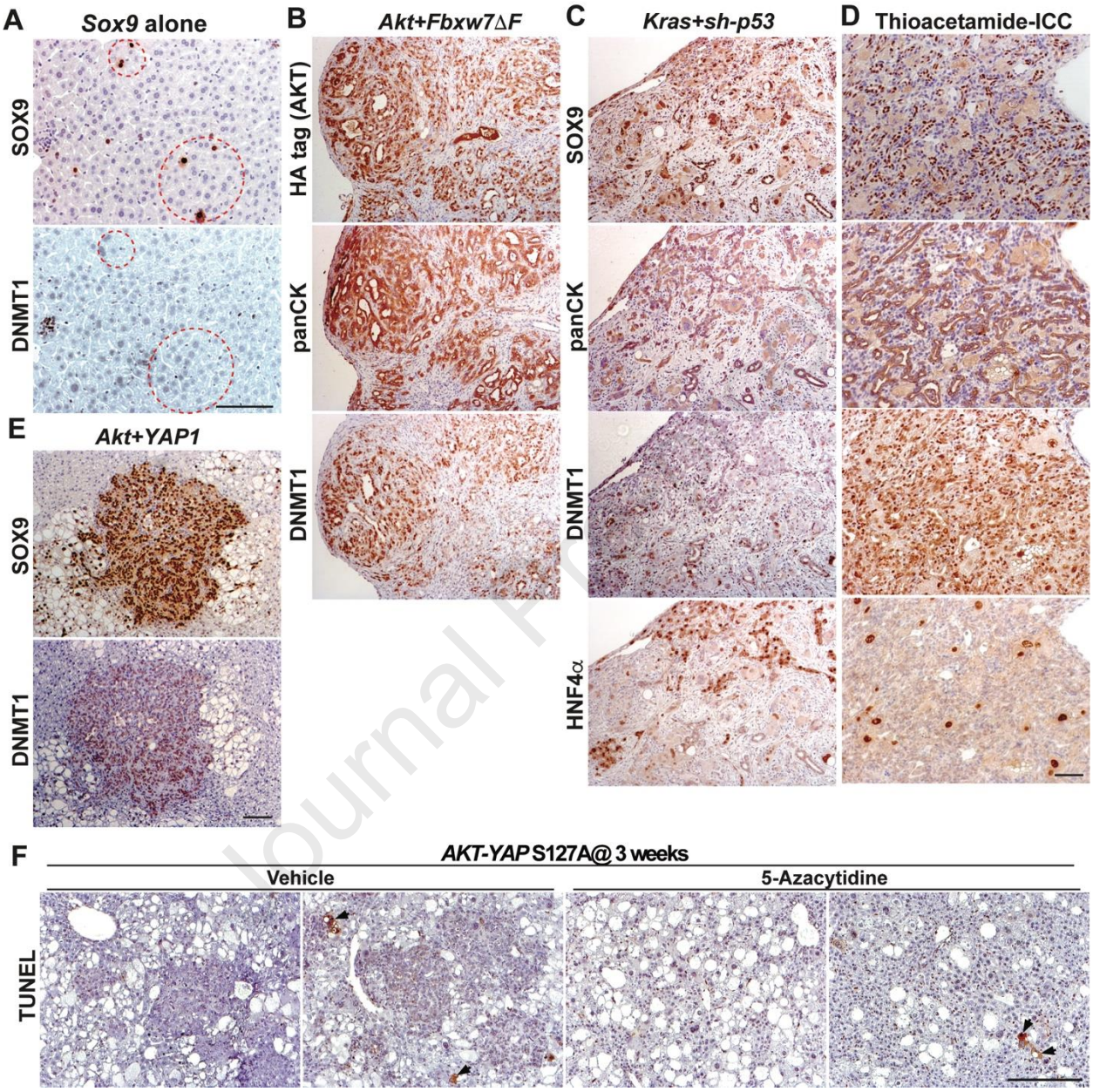

Figure S3. DNMT1 expression in HC-derived ICC models. (A) Representative IHC staining of *Sox9* expression plasmid-injected liver 3 weeks after injection showing absence of DNMT1 expression in *Sox9* singular-transduced HCs. **(B)** Representative IHC staining of liver from *Akt-Fbxw7ΔF*-driven ICC shows strong DNMT1 expression (100x). **(C)** Representative IHC staining of liver from *KRAS*-sh-*p53*-driven ICC shows strong

DNMT1 expression (100x). **(D)** Representative IHC staining of liver from *Akt-YAP*-driven ICC shows strong DNMT1 expression (100x). **(E)** Representative IHC staining of liver from TAA-administered mice at 24 weeks. IHC staining indicates panCK^{+};SOX9^{+};HNF4α^{-};DNMT1^{+} ICC with biliary morphology. **(F)** Representative TUNEL staining of liver from vehicle or 5-azacytidine-treated mice bearing *Akt-YAP1*-liver cancer at 3 weeks post HDTVI. Arrows indicate TUNEL^{+} cells. Scale bars:100 μm.

Figure S4

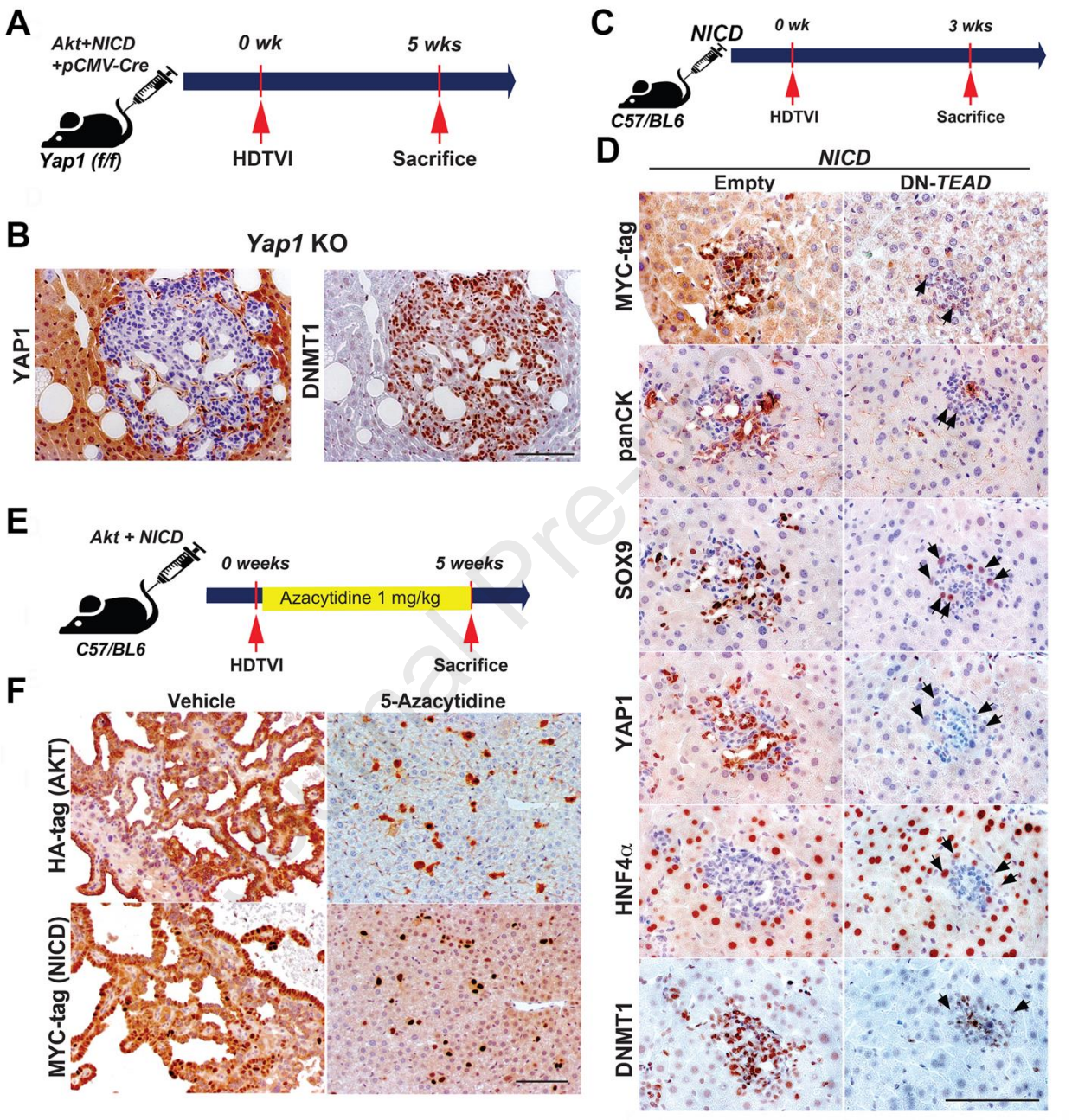

Figure S4. DNMT1 in HC-driven ICC. (A and B) Experimental design illustrating plasmids used for HDTVI, mice used in study and time-points analyzed. IHC staining for *Akt-NICD-Yap1* KO ICC at 5 weeks post HDTVI showing strong DNMT1 expression. **(C**

and D) Experimental design illustrating use of NICD alone or NICD + dn-TEAD plasmids for HDTVI and time-points analyzed. Representative IHC staining of *NICD-Empty* or *NICD*-DN-*TEAD* injected livers showing *NICD*-transfected cells (MYC-tag^{+}) with intact HC-to-ICC reprogramming with loss of HNF4α and gain of YAP, panCK and DNMT1. DN-*TEAD* livers showing *NICD*-transfected cells with defective HC-to-BEC reprogramming with continued HNF4α staining and absent of DNMT1 in YAP1^{-} HCs (black arrows). **(D)** Experimental design illustrating 5-Azacytidine treatment, plasmid used for HDTVI, mice used in study and time-point analyzed. **(E)** Representative IHC images for HA-tag (AKT), MYC-tag (NICD), and panCK showing dramatic tumor development in *Akt-NICD* WT livers and normal histology in 5-Azacytidine-treated livers at 5 weeks post HDTVI. Scale bars:100 µm.

Figure S5

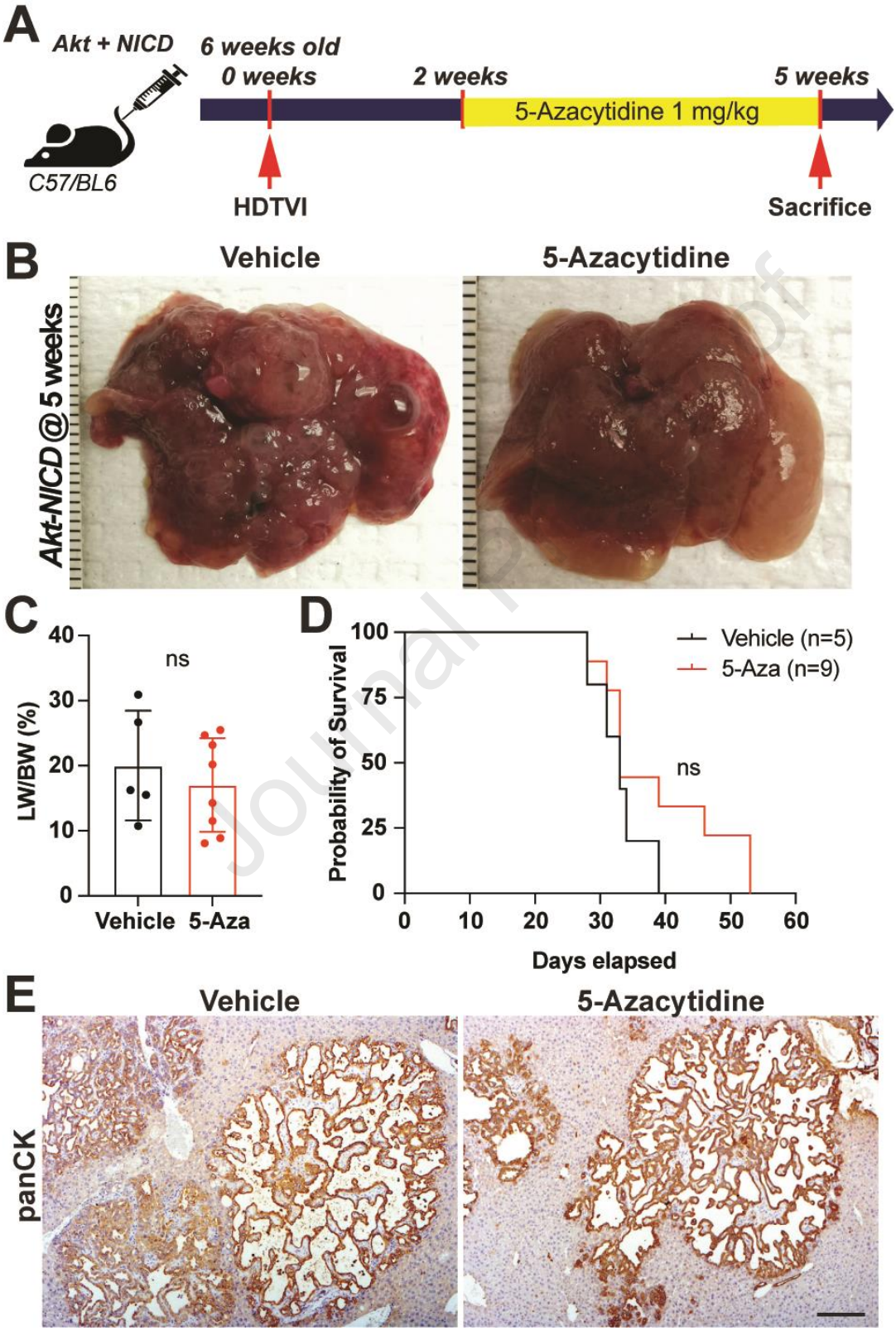

Figure S5: Pharmacologic DNMT1 inhibition does not reduce advanced AN-ICC tumor burden. (A) Experimental design illustrating 5-Azacytidine treatment, plasmids used for HDTVI, mice used in study and time-points analyzed. **(B)** Representative gross images show comparable *Akt-NICD* tumor development between Vehicle or 5-Azacytidine-treated livers at 5w post-injection **(C)** LW/BW ratio depicts comparable tumor burden in Vehicle or 5-Azacytidine-treated animals at 5w. **(D)** Kaplan-Meier survival curve showing comparable survival rate between Vehicle or 5-Azacytidine-treated mouse bearing AN-ICC**. (E)** Representative IHC images of 5w vehicle- or 5-Azacytidine-treated livers bearing *Akt-NICD*-driven ICC component positive for panCK. Ns, not significant; Scale bar: 100um.

Figure S6

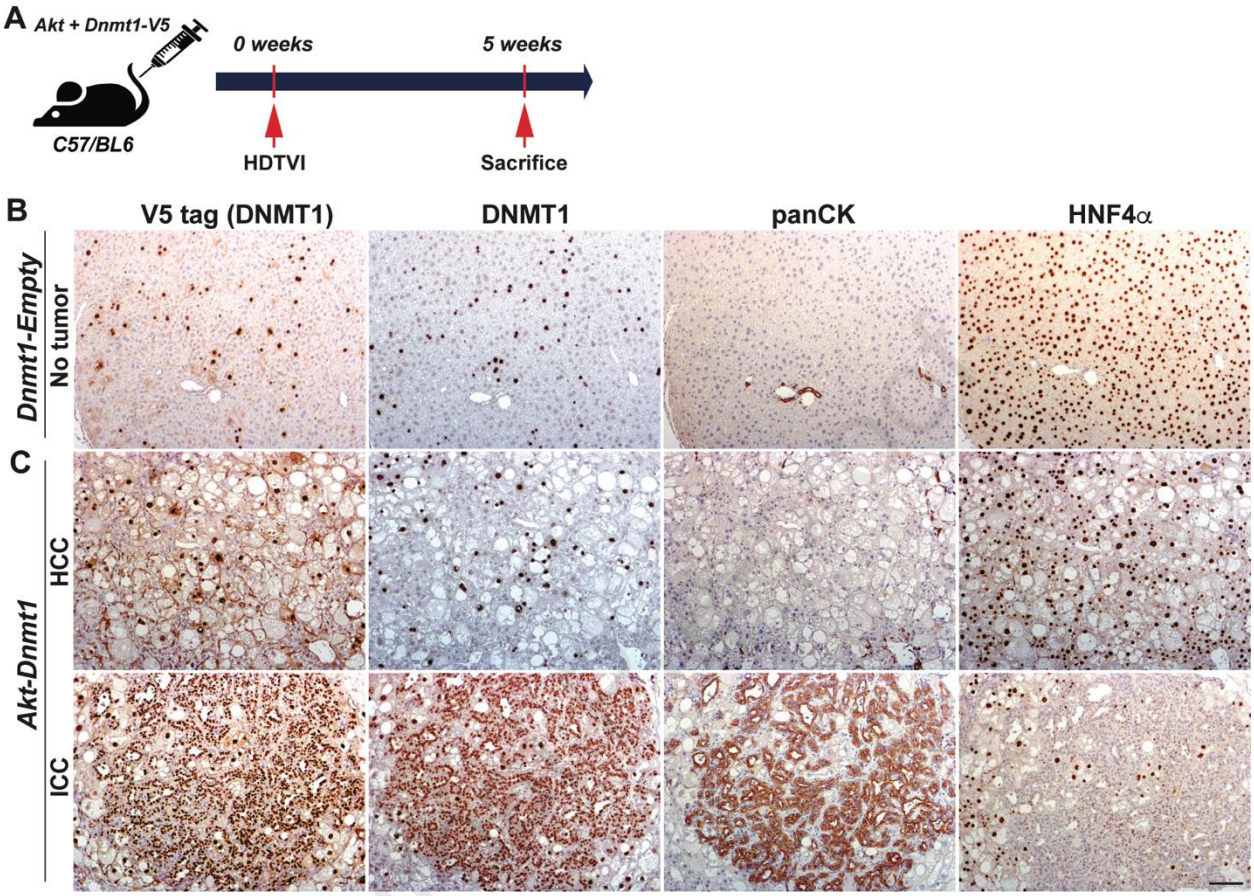

Figure S6: Concomitant expression of *mysAkt* and *Dnmt1* in a subset of murine HCs in vivo induces liver cancer development including ICC. **(A)** Experimental design illustrating plasmids used for HDTVI, mice used in study and time-points analyzed. **(C)** Representative IHC images of 5w *Akt-Dnmt1* show HCC and few ICC components to be positive. **(B)** In *Dnmt1-Empty* liver, no tumor was seen and all V5-tag^{+} cells retained HC morphology without clonal expansion. Scale bars: 100µm.

Figure S7

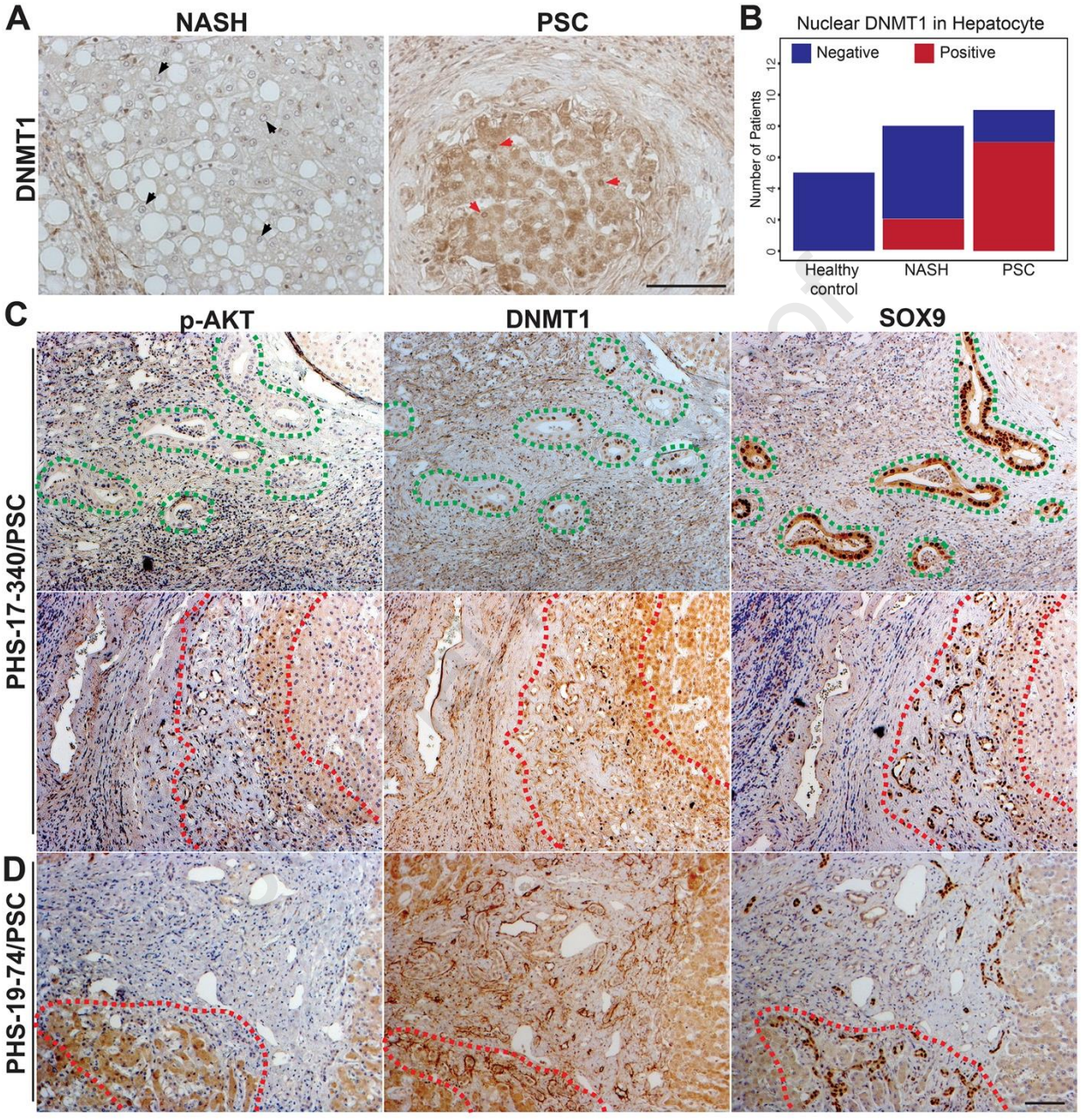

Figure S7. DNMT1 and p-AKT co-expression in PSC cases with ICC-like regions. **(A)** Representative IHC images of liver section from patients with PSC showing increased nuclear DNMT1 in HCs as compared to NASH or healthy liver. Black arrows point to DNMT1^{-} hepatocytes; red arrows to DNMT1^{+} hepatocytes. (**B**) Stacked-bar graph

showing higher incidence of nuclear DNMT1 in HCs in PSC patient livers compared with NASH and healthy livers. **(C and D)** Representative IHC images showing ICC-like premalignant foci in only a subset of PSC patient livers which also showed aberrant expression of p-AKT and DNMT1 in SOX9+ cells. Green dashed lines depicts $SOX9^{+}$;$DNMT1^{+}$;$p\text{-}AKT^{-}$ cells and Red dashed lines depicts $SOX9^{+}$;$DNMT1^{+}$;$p\text{-}AKT^{+}$ cells. Scale bars:100 µm